Quantum Coulomb systems : screening, recombination and van der Waals forces

Angel Alastuey

Quantum Coulomb systems : screening, recombination and van der Waals forces

A.Alastuey

Laboratoire de Physique, ENS Lyon and CNRS,

46 allée d'Italie, 69364 Lyon Cedex 07, France

(Dated: October 4, 2010)

Abstract

The study of quantum Coulomb systems at equilibrium is important for understanding properties of matter in many physical situations. Screening, recombination and van der Waals forces are basic phenomena which result from the interplay of Coulomb interactions, collective effects and quantum mechanics. Those phenomena are introduced in the first part of this lecture, through various physical examples. Their treatment within mean-field theories and phenomenological approaches is also exposed, while related predictions are discussed. This sheds light on fundamental issues, which must be analyzed without any *a priori* approximations or modelizations. The second part of this lecture is precisely devoted to the presentation of various exact results for the quantum proton-electron hydrogen plasma. Such results are derived within the Screened Cluster Representation, which is constructed by combining the path integral representation of the Coulomb gas with Mayer-like diagrammatical techniques. They illustrate the breakdown of Debye exponential screening by quantum fluctuations, as well as the emergence of familiar chemical species in suitable low-temperature and low-density limits. Also, the amplitude of van der Waals forces is shown to be reduced by free charges.

PACS numbers: 05.30.-d, 05.70.Ce, 52.25.Kn

I. INTRODUCTION

Under standard Earth conditions, and also in many astrophysical situations, the properties of matter result from the interplay between non-relativistic quantum mechanics and Coulomb interactions. All relativistic effects, as well as the other non-electromagnetic interactions can be safely omitted. A description of matter in terms of quantum nuclei and quantum electrons interacting *via* the Coulomb potential is then sufficient. In that context, the derivation of exact results for equilibrium properties of quantum Coulomb systems is of crucial importance.

The study of quantum Coulomb systems within statistical mechanics, requires to face several difficult problems related to both short- and long-range specificities of Coulomb potential, as well as to quantum mechanics itself, namely screening and recombination. In the first introductory part of the present lecture, those problems are successively adressed for various physical examples where free charges interacting *via* the Coulomb potential are present. First, it is instructive to consider screening in classical systems where quantum effects can be omitted. According to the pioneering Debye-like mean-field theories, Coulomb interactions are exponentially screened at the classical level, a prediction confirmed by a large variety of rigorous proofs and exact results. In the quantum case, similar mean-field theories also predict an exponential decay of equilibrium particle correlations. However, they do not account for a very fundamental feature of quantum mechanics, namely the intrusion of dynamical effects at equilibrium. Hence, there exist various arguments which suggest a breakdown of exponential screening in quantum systems. In the literature, recombination has been mainly dealt with in the framework of the chemical picture. The corresponding phenomenological approaches are based on *ad hoc* modelizations for preformed entities and their interactions.

As illustrated by the various considerations exposed in the introductory part of this lecture, screening, recombination and van der Waals forces result from entangled mechanisms combining Coulomb interactions and quantum mechanics. Although, phenomenological treatments of such phenomena have been widely developped, there still remain subtle effects, a deeper understanding of which requires a more funda-

mental analysis in the framework of quantum Coulomb systems, namely the so-called physical picture. The aim of the second part of this lecture is to present several exact results relative to fundamental issues about screening and recombination. For the sake of simplicity and pedagogy, we consider the quantum hydrogen plasma made with point protons and point electrons interacting *via* the Coulomb potential. First, we present rigorous proofs about thermodynamical stability on the one hand, and the atomic limit on the other hand. Then, we introduce the Feynman-Kac path integral representation, which turns out to be a quite efficient tool for our purpose. Its application to a many-body quantum system provides an equivalent classical system made with extended objects called loops. Standard Mayer-like diagrammatical series for the gas of loops, are exactly transformed into the Screened Cluster Representation for equilibrium quantities of the quantum system. That transformation, based on suitable resummations and reorganizations, accounts simultaneously for both screening and recombination. Quantum fluctuations, which play a crucial role in screening, are merely embedded in loop shapes. Recombination, which cannot be treated perturbatively in the Coulomb potential, is automatically ensured by the presence of Boltzmann factors associated with loop interactions. The Screened Cluster Representation is applied to hydrogen in the Saha regime, defined by both low temperatures and low densities, where it behaves as a partially ionized atomic gas. An exact asymptotic expansion for the equation of state is constructed, beyond familiar Saha theory. It sheds light on a suitable first-principles account of contributions of usual chemical species, without any *a priori* modelizations. Also, particle correlations are found to decay algebraically. Thus, ionized protons and ionized electrons only reduce the amplitude of van der Waals interactions between atoms. As a conclusion, we summarize the main answers to the above issues inspired by those exact results.

II. COULOMB INTERACTIONS AND QUANTUM MECHANICS AT WORK

A. Examples and specific features

A description of matter in terms of Coulomb systems, also called plasmas, is necessary as soon as free charges are present. There is a large variety of physical examples where such situations occur. For instance, electrolytes involve ionic species obtained by dissolution of salts into water. Also, in metals, the electrons of the conduction band freely move across the samples. Other examples can be found in astrophysical situations, where high temperatures or high pressures favor ionization of matter, in general inside the cores of compact objects or stars.

Let us consider a plasma made with point charges. Two charges q_i and q_j located at $\mathbf{r}_i$ and $\mathbf{r}_j$ interact *via* the instantaneous Coulomb potential

$$u_{\rm C}(\mathbf{r}_i, \mathbf{r}_j) = \frac{q_i q_j}{|\mathbf{r}_i - \mathbf{r}_j|} \ , \tag{II.1}$$

while the full interaction potential of the system reduces to the sum of pairwise interactions (II.1). Here, we dot not taken into account retardation effects or magnetic forces, and we discard the coupling of charges to elecromagnetic radiation. That purely Coulombic description is sufficient as far as the average speed of charges is small compared to the speed of light c. Roughly speaking, for a classical charge with mass m, this requires that the thermal energy $k_B T$ is small compared to the rest energy mc^2 [74]. This implies $T \ll 10^{10} K$ for electrons and $T \ll 10^{13} K$ for protons. Such conditions are fullfilled in many physical systems!

Contrarily to interactions between neutral entities, Coulomb potential is long ranged, namely it is not integrable at large distances

$$\int_{r>D} {\rm d}\mathbf{r} \, \frac{1}{r} = \infty \ , \tag{II.2}$$

where D is some irrelevant cut-off length. That divergence might pollute thermodynamical quantities, and usual extensivity properties might be lost. The underlying physical picture is that charges with the same sign tend to repell together too strongly at large distances, so the system might explode.

In addition to above long-range problems, the $1/r$-nature of the Coulomb potential causes also some trouble at short distances. If we consider two classical opposite point charges $\pm q$ separated by a distance r, the corresponding Boltzmann factor is not integrable at $r = 0$, *i.e.*

$$\int_{r<D} \mathrm{d}\mathbf{r} \, \exp\left(\frac{\beta q^2}{r}\right) = \infty \tag{II.3}$$

with $\beta = 1/(k_B T)$. Thus, a classical system with positive and negative point charges collapses.

According to above considerations, the study of Coulomb systems in the framework of statistical mechanics has to face two central difficulties related to the behaviours of the Coulomb potential at respectively large ($r \to \infty$) and short ($r \to 0$) distances. In the following, we will describe the fundamental mechanisms which cure the corresponding singularities, namely screening and recombination. Screening is a collective effect which prevents explosion at large distances. Recombination is a purely quantum mechanical effect, where the uncertainty principle smears out the divergency of the Coulomb potential at $r = 0$, so collapse is avoided. Those mechanisms are adressed successively, by considering physical systems for which simplified models and/or phenomenological approaches can be introduced.

First, in Section II B, we present Debye theory for a classical electrolyte. That mean-field approach predicts an exponential screening of Coulomb interactions, which is confirmed by rigorous results. A similar mean-field theory has been applied to the quantum electron gas, as described in Section II C. Again, an exponential screening is found, but that prediction is shown to be quite doubtful according to the unavoidable intrusion of dynamical effects in equilibrium quantities of quantum systems. Recombination and van der Waals forces are considered in Section II D through the example of hydrogen in the Sun, the state of which changes from a fully ionized plasma in the core to an atomic gas in the photosphere. We present simple arguments, as well as some standard phenomenological considerations, which introduce the more sophisticated analysis presented in the second part of this lecture.

B. Screening in classical systems

1. *Primitive model for an electrolyte*

Let us consider an ordinary solution of sodium chloride. For a concentration $C_0 = 0.1$ moles/l at room temperature $T = 300$ K, the salt is entirely dissociated, so the solution reduces to a mixture of ions Na^+, Cl^- and water molecules H_2O (ions H_3O^+ and OH^- are omitted since their concentration is negligible compared to C_0). The mean interionic distance, $a = (3/(4\pi\rho))^{1/3}$ with the common ionic number densities $\rho = \rho_+ = \rho_-$, is large compared to both the typical size d of ions and the mean distance between water molecules. Therefore, a large number of water molecules surrounds each ion, and water may be reasonably replaced by a continuous medium with dielectric constant ϵ_w. Also the de Broglie thermal wavelengths $\lambda_\pm = (\beta\hbar^2/M_\pm)^{1/2}$ are small compared to d, so ions can be treated classically.

According to the above hierarchy of length scales, the present electrolytic solution is well described by a classical two-component plasma made with hard spheres carrying charges $q_\pm = \pm e$, also called the restrictive primitive model in the literature. Two ions of species $\alpha = \pm$ and $\gamma = \pm$ separated by a distance r interact *via* the potential

$$\begin{aligned} u_{\alpha\gamma}(r) &= +\infty \ , \ r < d_{\alpha\gamma} \\ u_{\alpha\gamma}(r) &= \frac{q_\alpha q_\gamma}{\epsilon_w r} \ , \ r > d_{\alpha\gamma} \ . \end{aligned} \tag{II.4}$$

The hard-core part of the potential is a phenomenological description of the short-range repulsion between the electronic clouds of the two considered ions. Of course, within that modelization, no collapse between oppositely charged ions occur. Also, notice that the bare Coulomb potential is renormalized *via* the standard factor $1/\epsilon_w$ which accounts for the underlying presence of a continuous dielectric medium.

In order to adress the question of screening, we introduce the equilibrium charge density $C_\alpha(\mathbf{r})$ surrounding an ion with species α fixed at the origin, which reads

$$C_\alpha(\mathbf{r}) = \sum_\gamma q_\gamma \frac{\rho^{(2)}_{\alpha\gamma}(\mathbf{0}, \mathbf{r})}{\rho_\alpha} \tag{II.5}$$

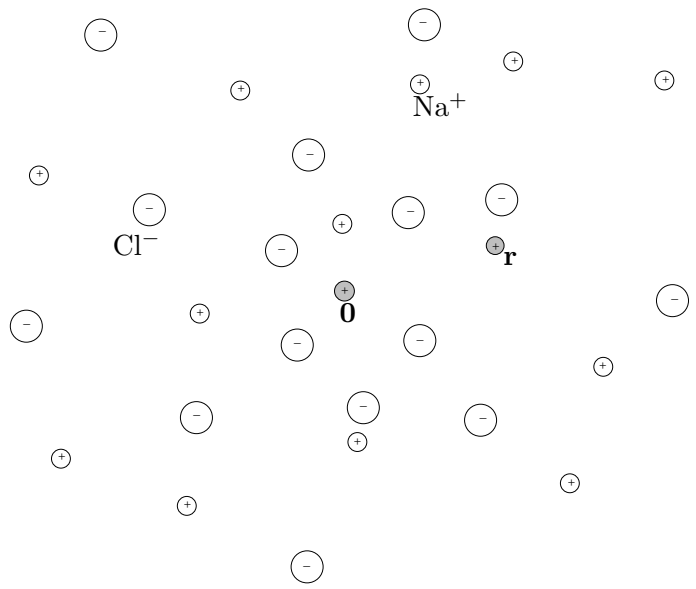

FIG. 1: A typical ionic configuration $\mathcal{C}$ where two cations Na^+ ($\alpha = \gamma = +$) are fixed at $\mathbf{0}$ and $\mathbf{r}$ respectively.

where $\rho^{(2)}_{\alpha\gamma}$ is the two-point equilibrium distribution of species α and γ. Screening can be easily understood within a mean-field calculation of $C_\alpha(\mathbf{r})$. The basic ideas sustaining mean-field approach have been first introduced by Gouy [1] and Chapman [2] fot the study of electrical double layers near charged electrodes. They have been extended to the calculation of polarization clouds in the bulk phase by Debye and Huckel [3]. Here, we present the corresponding arguments which provide the mean-field form of $C_\alpha(\mathbf{r})$.

2. Debye theory

Let $\mathcal{C}$ be a given spatial configuration of ions where one ion α is fixed at the origin and one ion γ is fixed at $\mathbf{r}$. In Fig. 1, we draw a typical configuration which illustrates that ion α attracts oppositely charged ions and repells the other ones. Ion γ feels the electrostatic potential $\varphi(\mathbf{r}|\mathcal{C})$ created at $\mathbf{r}$ by all the remaining ions, in particular those which are far apart, because the Coulomb potential is long ranged. Since $\varphi(\mathbf{r}|\mathcal{C})$ is a sum of a large number of terms, fluctuations of the positions of non-fixed ions should slightly modify its value. That statement is inspired by the law of large numbers, and it can been applied to other many-body problems where

long range interactions are present [75]. Thus, it is tempting to replace $\varphi(\mathbf{r}|\mathcal{C})$ by its average value $\varphi_\alpha(\mathbf{r})$, which is nothing but the electrostatic potential created by ion α plus its polarization cloud with charge distribution $C_\alpha(\mathbf{r})$. Within that mean-field treatment, the density of ions γ at $\mathbf{r}$ is merely given by the Boltzmann distribution of an ideal gas in the external potential $q_\gamma\varphi_\alpha(\mathbf{r})$, *i.e.*

$$\frac{\rho^{(2)}_{\alpha\gamma}(\mathbf{0},\mathbf{r})}{\rho_\alpha} = \rho_\gamma \exp(-\beta q_\gamma \varphi_\alpha(\mathbf{r}))\,. \tag{II.6}$$

At this level, we have completely omitted short-range effects arising from the hard-core part of ion-ion potential (II.4). Under diluted conditions for which $d \ll a$, this is legitimate since for most configurations $\mathcal{C}$, ion γ only feels the Coulomb parts of its interactions with other ions. At the same time, position fluctuations of neighbours of fixed ion γ can be neglected, only if they generate variations of $\varphi(\mathbf{r}|\mathcal{C})$ which do not exceed the thermal energy k_BT. This implies that the corresponding typical value $e^2/(\epsilon_{\rm w}a)$ of Coulomb interactions is small compared to k_BT, a condition indeed fulfilled at low densities. According to previous considerations, the linearization of the Boltzmann factor (II.6) is consistent with the mean-field treatment, and it provides

$$C_\alpha(\mathbf{r}) = -\beta \sum_\gamma q_\gamma^2 \rho_\gamma \varphi_\alpha(\mathbf{r})\,, \tag{II.7}$$

where we have used the neutrality condition

$$\sum_\gamma q_\gamma \rho_\gamma = 0\,. \tag{II.8}$$

The insertion of the linearized expression (II.7) of $C_\alpha(\mathbf{r})$ into Poisson equation for $\varphi_\alpha(\mathbf{r})$, shows that $\varphi_\alpha(\mathbf{r}) = q_\alpha\phi_{\rm D}(\mathbf{r})$, where $\phi_{\rm D}$ is the solution of

$$\left(-\Delta + \kappa_{\rm D}^2\right)\phi_{\rm D}(\mathbf{r}) = \frac{4\pi}{\epsilon_{\rm w}}\,\delta(\mathbf{r}) \tag{II.9}$$

with

$$\kappa_{\rm D}^2 = \frac{4\pi}{\epsilon_{\rm w}}\beta\sum_\gamma q_\gamma^2\rho_\gamma = \frac{8\pi}{\epsilon_{\rm w}}\beta e^2\rho \tag{II.10}$$

and boundary conditions

$$\phi_{\rm D}(\mathbf{r}) \to 0 \quad \text{when} \quad r \to \infty\,. \tag{II.11}$$

Such boundary conditions amount to impose that the ionic densities induced at $\mathbf{r}$ tend to the bulk homogeneous value ρ when $r \to \infty$, or in other words to make the quite plausible assumption that polarization effects decay at large distances.

The Helmholtz equation (II.9) together with boundary conditions is easily solved in Fourier space, and $\phi_{\rm D}(\mathbf{r})$ is then readily obtained by applying Cauchy's theorem (see *e.g.* Ref. [6] for a detailed presentation of that standard calculation),

$$\phi_{\rm D}(\mathbf{r}) = \phi_{\rm D}(r) = \frac{\exp(-\kappa_{\rm D} r)}{\epsilon_{\rm w} r} \ . \tag{II.12}$$

Thus, the electrostatic potential $q_\alpha \phi_{\rm D}(r)$ inside the electrolytic solution decays exponentially faster than the potential $q_\alpha/(\epsilon_{\rm w} r)$ created by a single ion α immersed in water. In the electrolyte, such an ion is screened by its induced polarization cloud over the so-called Debye length $\lambda_{\rm D} = \kappa_{\rm D}^{-1}$.

3. Reliability and limits of mean-field predictions

It is instructive to determine what are the physical conditions under which the mean-field treatment is reliable at a quantitative level. The main argument for neglecting fluctuations relies on the large value of the number of ions which contribute to the electrostatic potential at $\mathbf{r}$. In average, those ions are contained in a sphere with radius r as a consequence of Gauss theorem, so their number is of order $8\pi\rho r^3/3$. That number must be large for r of order the typical length scale $\lambda_{\rm D}$. This implies $a\kappa_{\rm D} \ll 1$, or equivalently the weak-coupling condition $e^2/(\epsilon_{\rm w} a k_B T) \ll 1$. Within that condition, the linearization of Boltzmann factor (II.6) is also justified. If that condition is fulfilled at high temperatures or low densities, hard-core effects can be neglected only if $d \ll a$. The previous mean-field approach is then expected to be valid, at least at a quantitative level, at sufficiently high temperatures and low densities. Notice that in the present example, the weak-coupling condition is ensured thanks to the large value of the water dielectric constant, $\epsilon_{\rm w} \simeq 80$, which drastically reduces the strength of electrostatic interactions. As a consequence, Debye theory works reasonably well for most electrolytic solutions of ordinary salts under standard conditions.

Beyond its practical interest for a large variety of physical systems, Debye theory suggests a fundamental result, namely the exponential decay of correlations in classical charged systems, at least in fluid phases. In fact, that remarkable property has been proved for various systems [7–9] at sufficiently high temperatures and sufficiently low densities, *i.e.* in thermodynamical regimes where mean-field approach is expected to work. The very difficult part of those proofs relies on the complete control of the contributions of all the effects omitted in Debye theory. It turns out that such effects do not destroy the exponential clustering predicted by mean-field. In other words, the essence of classical exponential screening is captured by mean-field approach, which enlights its collective nature. Also, the harmonicity of the Coulomb potential is a key ingredient, as illustrated by an analysis of the equilibrium BGY hierarchy [10]. In general, the fast decay of particle correlations is proved to be related to a perfect arrangment of polarization clouds, as exemplified through multipole sum rules [11]. Here, the total charge of the polarization cloud surrounding α must exactly cancel out its charge, namely

$$\int \mathrm{d}\mathbf{r}\; C_\alpha(\mathbf{r}) = -q_\alpha \; . \tag{II.13}$$

That monopole sum rule is indeed satisfied by the mean-field expression

$$-\, q_\alpha \kappa_{\mathrm{D}}^2 \frac{\exp(-\kappa_{\mathrm{D}} r)}{4\pi r} \tag{II.14}$$

of $C_\alpha(\mathbf{r})$. Of course, the existence of positive and negative charges is crucial for screening of Coulomb interactions [76]. The mean-field expression (II.14) diverges when $r \to 0$. Such divergency is unphysical, and it proceeds from the linearization of Boltzmann factor (II.6) which is never valid at short distances. However, that spurious short-range singularity does not affect integrated quantities, like the total charge (II.13) or thermodynamical quantities.

At a quantitative level, corrections to Debye theory can be derived within Abe-Meeron diagrammatical expansions [14, 15]. Debye theory is merely recovered by keeping only the first graph in those series. Each of the remaining graphs provides an exponentially decaying contribution to particle correlations, in agreement with above proofs. The resulting screening length $\lambda_{\mathrm{S}}(\rho, T)$ differs from its Debye expression λ_{D}, and it might be approximately estimated by selecting suitable classes of Abe-Meeron

graphs. Notice that short-range repulsion contributes to $\lambda_{\rm S}(\rho,T)$ in a rather subtle way, so a reliable description of the variations of $\lambda_{\rm S}(\rho,T)$ when temperature is decreased and/or density is increased is a challenging problem. At sufficiently low temperatures and/or high densities, the occurence of phase transitions might lead to divergencies of $\lambda_{\rm S}(\rho,T)$. For instance, exponential screening might be lost in a crystalline phase, or at the critical point of the liquid-gas transition as suggested in Ref. [16].

Eventually, let us conclude that section by a very important remark about dynamical aspects. In a real sample, ions continuously move, and because of their finite inertia, instantaneous perfect arrangments of the polarization clouds cannot be ensured. However, according to the somewhat magical recipe of statistical mechanics, at equilibrium the time-average of any quantity can be equivalently computed as a phase-space average with the Gibbs measure. Thanks to the remarkable factorization of that measure into the Maxwellian distribution of momenta times the Boltzmann factor associated with the interaction potential, dynamical features are washed out by momenta integration. Then, the calculation of equilibrium correlations in position space becomes a purely static problem, where only configurations of particle positions must be considered without caring about particle velocities. In other words, dynamical fluctuations no longer intervene, so above considerations about particle inertia are not relevant. However, in a quantum system where above factorization of the Gibbs measure is no longer valid, we can anticipate that dynamical effects should contribute to equilibrium correlations.

C. Screening in quantum systems

1. Jellium model for conduction electrons

In ordinary metals, like Copper for instance, there exists a finite density ρ of ionized electrons which ensure electrical conduction. Those electrons freely move among the remaining ions, which can be considered as fixed at their lattice sites. A further simplification is to replace the periodic ionic charge density by the constant $e\rho$. This provides a model for conduction electrons, called either jellium or one-

component plasma, where such electrons are immersed in an uniform and rigid neutralizing background.

Under standard conditions and for simple metals with one or two ionized electrons per atom, the typical values for temperature and density are $T = 300$ K and $\rho = 3.10^{28}$ m^{-3}. The thermal de Broglie wavelength of electrons $\lambda_{\rm e} = (\beta\hbar^2/m_{\rm e})$ is then large compared to the mean interelectronic distance $a = (3/(4\pi\rho))^{1/3}$, so electrons must be described by quantum mechanics. Equivalently, thermal energy k_BT is small compared to Fermi energy $\varepsilon_{\rm F} = \hbar^2 k_{\rm F}^2/(2m_{\rm e})$ with Fermi wavenumber $k_{\rm F} = (3\pi^2\rho)^{1/3}$, so electrons are strongly degenerate and their typical kinetic energy is of order $\varepsilon_{\rm F}$. Since $\varepsilon_{\rm F}$ is small compared to the rest energy $m_{\rm e}c^2$, relativistic effects can be omitted. Therefore, we have to consider the non-relativistic quantum version of jellium, where two electrons separated by a distance r interact *via* the instantaneous Coulomb potential

$$u_{\rm ee}(r) = \frac{e^2}{r} \ . \tag{II.15}$$

In addition, each electron is submitted to the electrostatic potential created by the ionic background, while the constant background self-electrostatic energy is also taken into account in the full interaction potential of the system. Electrons obey to Fermi statistics since they carry an half-integer spin. Notice that the Coulomb Hamiltonian of the present model do not depend on electron spins.

2. Thomas-Fermi theory

Similarly to the classical case described above, screening properties can be merely illustrated through a mean-field calculation of the equilibrium charge density $C_{\rm e}(\mathbf{r})$ surrounding an electron fixed at the origin,

$$C_{\rm e}(\mathbf{r}) = -e\left(\frac{\rho_{\rm ee}^{(2)}(\mathbf{0},\mathbf{r})}{\rho} - \rho\right) \ . \tag{II.16}$$

In definition (II.16), $\rho_{\rm ee}^{(2)}$ is the two-point equilibrium distribution of electrons, while the substracted term accounts for the ionic background density. The so-called Thomas-Fermi theory [17, 18] was introduced for describing the electronic structure of atoms, and it can be viewed as the source of further density functional methods.

Its application to the study of screening properties [19] can be rephrased similarly to the mean-field approach for the classical case. Namely, we assume that the electrons close to a given point $\mathbf{r}$ constitute an ideal gas submitted to the external one-body potential $-e\varphi_{\rm e}(\mathbf{r})$, where $\varphi_{\rm e}(\mathbf{r})$ is nothing but the electrostatic potential created by the electron fixed at the origin plus its polarization cloud with charge distribution $C_{\rm e}(\mathbf{r})$. Now, according to the quantum nature of that ideal gas, its density is related to the external potential *via* the Fermi-Dirac distribution instead of the Boltzmann law, *i.e.*

$$\frac{\rho_{\rm ee}^{(2)}(\mathbf{0},\mathbf{r})}{\rho} = \frac{2}{(2\pi)^3}\int {\rm d}\mathbf{k}\,\frac{1}{\exp[\beta(\varepsilon(\mathbf{k})-e\varphi_{\rm e}(\mathbf{r})-\mu)]+1}\,. \tag{II.17}$$

In Fermi-Dirac expression (II.17), $\varepsilon(\mathbf{k}) = \hbar^2k^2/(2m_{\rm e})$ is the non-relativistic kinetic energy of a plane wave with wavenumber $\mathbf{k}$, while the chemical potential μ, taken constant across the system, is naturally determined by the bulk condition

$$\rho = \frac{2}{(2\pi)^3}\int {\rm d}\mathbf{k}\,\frac{1}{\exp[\beta(\varepsilon(\mathbf{k})-\mu)]+1}\,. \tag{II.18}$$

Assuming that polarization effects vanish at large distances, we set $\rho_{\rm ee}^{(2)}(\mathbf{0},\mathbf{r}) \to \rho^2$ when $r \to \infty$. The corresponding limit form of equation (II.17) then implies the boundary condition $\varphi_{\rm e}(\mathbf{r}) \to 0$.

As argued for the Boltzmann factor involved in Debye theory, the linearization of Fermi-Dirac distribution (II.17) with respect to $\varphi_{\rm e}(\mathbf{r})$, is consistent with the present mean-field treatment, which also requires that Coulomb interactions are small perturbations. If we set $\varphi_{\rm e}(\mathbf{r}) = -e\phi_{\rm TF}(\mathbf{r})$, we then obtain an Hemholtz equation for $\phi_{\rm TF}(\mathbf{r})$ which is identical to its classical counterpart (II.9) for $\phi_{\rm D}(\mathbf{r})$, except for the replacements $\epsilon_{\rm w} \to 1$ and $\kappa_{\rm D} \to \kappa_{\rm TF}$ where the Thomas-Fermi wavenumber $\kappa_{\rm TF}$ is defined by

$$\kappa_{\rm TF}^2 = 4\pi e^2\frac{\partial\rho}{\partial\mu}(\beta,\mu)\,. \tag{II.19}$$

The resulting mean-field expression for charge distribution $C_{\rm e}(\mathbf{r})$ reads

$$-e\kappa_{\rm TF}^2\frac{\exp(-\kappa_{\rm TF}r)}{4\pi r}\,. \tag{II.20}$$

Thus, the mean-field approach again predicts an exponential screening. Now the screening length $\lambda_{\rm TF}$ takes into account degeneracy effects controlled by dimensionless parameter $\varepsilon_{\rm F}/k_BT$. In the limit of weak degeneracy, which can be obtained by

setting $\mu \to -\infty$ at fixed β, the density vanishes as $\rho \sim 2\exp(\beta\mu)/(2\pi\lambda_{\rm e})^{3/2}$, so $\lambda_{\rm TF}$ does reduce to its classical Debye form $(4\pi\beta e^2\rho)^{-1/2}$. In the opposite strong-degeneracy limit, obtained by setting $\mu \to +\infty$ at fixed β, the density diverges as $\rho \sim (2m_{\rm e}\mu)^{3/2}/(3\pi^2)$ and we find

$$\lambda_{\rm TF} \sim \left(\frac{\pi^2}{144}\right)^{1/6} \left(\frac{\hbar^2 a}{m_{\rm e}e^2}\right)^{1/2} . \tag{II.21}$$

3. Expected validity regime

As quoted above, the validity of Thomas-Fermi theory requires weak-coupling conditions. Of particular interest is the regime of strong degeneracy, where the relevant kinetic energy is the Fermi energy $\varepsilon_{\rm F}$. The corresponding weak-coupling condition reads $e^2/(a\varepsilon_{\rm F}) \ll 1$. That strongly-degenerate weakly-coupled regime is reached at sufficiently high densities for a given temperature. Indeed, when $\rho \to +\infty$ at fixed β, Fermi energy obviously becomes larger than classical thermal energy, while Coulomb energy of order $\rho^{1/3}$ grows slower than kinetic Fermi energy of order $\rho^{2/3}$. In that high-density limit, notice that $\lambda_{\rm TF}$, given by expression (II.21), becomes large compared to a, so the number of electrons inside the screening sphere with radius $\lambda_{\rm TF}$ is indeed large.

In order to derive corrections to the mean-field approach, it is necessary to use the formalism of many-body perturbation theory [20]. In that framework, the mean-field ideas are recasted into the celebrated Random Phase Approximation (RPA), which is close to Thomas-Fermi theory. In particular, RPA also predicts an exponential decay of charge correlations. Systematic corrections to RPA can be derived by taking into account suitable Feynman graphs. This leads to asymptotic high-density expansions of thermodynamical quantities, like the pressure or the internal energy, beyond their ideal strongly-degenerate forms.

For the strongly-degenerate electron gas described above, the Coulomb energy is not small compared to the Fermi energy. Therefore the system is not weakly coupled, and the application of Thomas-Fermi theory is rather questionable. In particular, we find that $\lambda_{\rm TF} \simeq 0.1$ nm is smaller than $a \simeq 0.2$ nm, in violation of the mean-field validity condition $\lambda_{\rm TF} \gg a$ [77].

4. Doubts about mean-field predictions

If mean-field approaches like RPA may provide the leading behaviour of integrated quantities involving $C_{\rm e}(\mathbf{r})$ in the high-density limit $\rho \to +\infty$ at fixed β, their reliability for $C_{\rm e}(\mathbf{r})$ itself is not uniform with respect to distance r. At short distances, the divergency of Thomas-Fermi expression (II.20) for $C_{\rm e}(\mathbf{r})$ is obviously unphysical, like for its classical counterpart in the framework of Debye theory. This is due first to the strong repulsion embedded in $\varphi_{\rm e}(\mathbf{r})$ when $r \to 0$ which cannot be treated perturbatively. Also TF theory does not account for the effective repulsion induced by Pauli principle when both electrons located at $\mathbf{0}$ and $\mathbf{r}$ have the same spin orientations. At large distances, and contrarily to the classical case, mean-field predictions are also doubtful, as argued below.

In writing the Fermi-Dirac distribution (II.17), a very important implicit assumption is made. Indeed, potential $\varphi_{\rm e}(\mathbf{r})$ is treated as a constant, so the energy levels are merely shifted by that constant from their corresponding purely kinetic expression $\varepsilon(\mathbf{k}) = \hbar^2 k^2/(2m_{\rm e})$. This amounts to neglect the spatial variations of $\varphi_{\rm e}(\mathbf{r})$, or in other words to omit diffraction effects arising from the non-commutativity of the kinetic and potential parts of Hamiltonian $-\hbar^2\Delta/(2m_{\rm e}) + \varphi_{\rm e}(\mathbf{r})$. Then, we are left with a purely configurational static problem, like in the classical case, and not surprisingly this leads also to an exponential screening. However, that result is rather questionable since an intrinsic specificity of quantum mechanics has been erased from the start!

The occurence of quantum diffraction in equilibrium statistical weights is a signature of dynamical effects, which are consequently still present at equilibrium. Now, and contrarily to the classical case, dynamical fluctuations combined to inertia effects should prevent instantaneous perfect arrangments of equilibrium screening clouds. Thus, the presence of partially screened multipolar interactions can be anticipated, and this might lead to a breakdown of exponential screening in equilibrium correlations. That quite plausible scenario has been first conjectured in Ref. [22], according to the presence of algebraic tails in some imaginary-time Green functions. Notice that an analogous scenario occurs for classical time-displaced correlations [23].

D. Recombination and van der Waals interactions

1. *Hydrogen in the Sun*

The sun is mainly made of hydrogen and helium, while heavier elements like oxygen, carbon, iron,...are less abundant and contribute to a small fraction of its total mass. Here, we will focus our study on hydrogen, and we will discard its interactions with all the other elements. Also, we do not consider complicated phenomena at work inside the Sun, like radiation transfer or convection for instance. For our purpose, it is sufficient to assume that some local thermodynamical equilibrium is reached at any place, and then the central question is to determine the corresponding chemical composition of an hydrogen plasma in terms of ionized and recombined entities.

In the core of the Sun, temperature T is of the order of 10^6 K and density ρ is of order 1 g/cc. Since $k_BT \simeq 90$ eV is much larger than the Rydberg energy of order 13.6 eV, atoms, molecules, as well as other recombined entities are then fully ionized. The hydrogen gas is then mainly composed of free protons and of free electrons. In intermediate layers, temperature and density decrease as the distance to the core increases. This favors recombination of protons and electrons into atoms, and hydrogen then behaves as a partially ionized atomic gas. In the photosphere, T is of order 6.10^3 K while ρ is of order 10^{-7} g/cc. Under such cool ($k_BT \simeq 0.5$ eV much smaller than Rydberg energy) and diluted (the mass density of Earth atmosphere is of order 10^{-3} g/cc) conditions, the full proton-electron recombination is achieved, and hydrogen reduces to an atomic gas. That recombination process is schematically represented in Fig. 2.

A proper description of above recombination process within statistical mechanics requires to account for both quantum mechanics and Coulomb interactions as detailed in the next Section. Here, we list several natural problems, and we present simple preliminary arguments which are particularly useful for a better understanding of more sophisticated analysis carried out in the framework of the many-body problem.

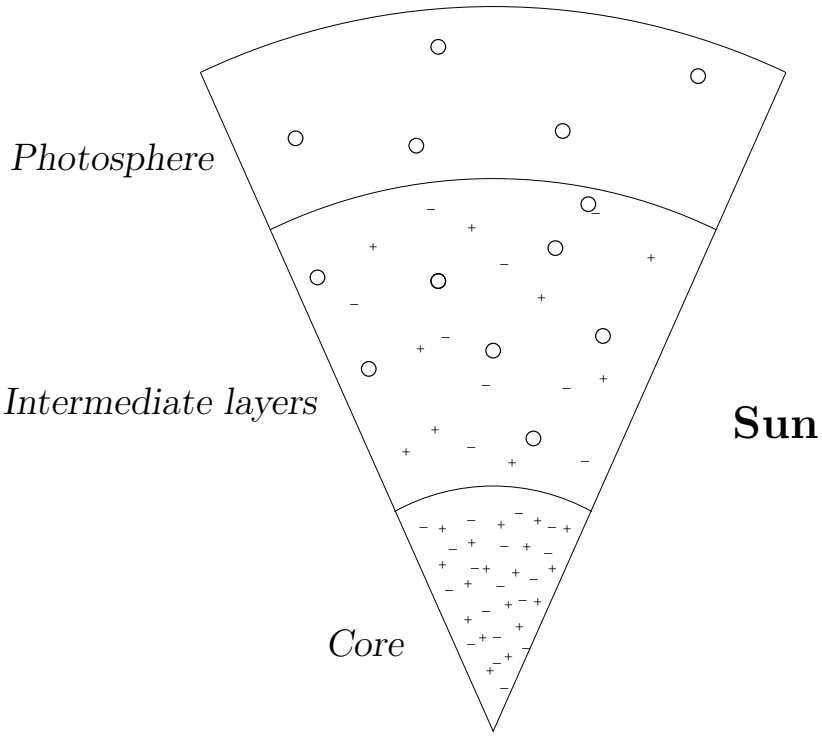

FIG. 2: A schematic view of the Sun. Signs + and − represent ionized protons and ionized electrons respectively, while circles represent hydrogen atoms.

2. How to define an hydrogen atom?

In quantum mechanics, all particle positions are entangled in a global wavefunction describing the whole system. If we consider an eigenfunction of the total Hamiltonian, no two-body wavefunction describing an hydrogen atom can be factored out. In that context, an unambiguous definition of such an atom is only possible in the double limit $\rho \to 0$ and $T \to 0$. Indeed, the zero-density limit ensures that once a proton has married an electron, all other neighbours are very far apart. Also, the zero-temperature limit guarantees that the atom stays in its groudstate and no thermal ionization occurs. Under such infinitely diluted and cold conditions, it can be reasonably expected that a single hydrogen atom in the vacuum naturally emerges.

3. How protons and electrons recombine into atoms?

The formation of atoms in a gas of protons and electrons has been studied long ago by Saha [24], in the framework of the chemical picture. He considered protons,

electrons and atoms as three independent species with their own chemical potentials. If all interactions are neglected and if each species is viewed as a classical ideal gas, the mass action law associated with the recombination equation $\mathrm{p} + \mathrm{e} \rightleftharpoons \mathrm{H}$, reads in terms of species ideal densities

$$\frac{\rho_{\mathrm{p}}^{(\mathrm{id})} \rho_{\mathrm{e}}^{(\mathrm{id})}}{\rho_{\mathrm{at}}^{(\mathrm{id})}} = \frac{\exp(\beta E_{\mathrm{H}})}{(2\pi\lambda_{\mathrm{pe}}^2)^{3/2}} \, , \tag{II.22}$$

where E_{H} is the groundstate energy of an hydrogen atom, $E_{\mathrm{H}} = -me^4/(2\hbar^2)$, with reduced mass $m = (m_{\mathrm{p}} m_{\mathrm{e}})/(m_{\mathrm{p}} + m_{\mathrm{e}})$ and associated de Broglie wavelength $\lambda_{\mathrm{pe}} = (\beta\hbar^2/m)^{1/2}$. The temperature-dependent reaction constant in the r.h.s. of mass action law (II.22), goes to zero when T vanishes, while it explodes when T diverges. Therefore, and as expected, low temperatures favor atomic recombination, while high temperatures favor ionization.

At given temperature and density, the chemical composition of the hydrogen gas is determined by adding to mass action law (II.22) the neutrality rule, $\rho_{\mathrm{p}}^{(\mathrm{id})} = \rho_{\mathrm{e}}^{(\mathrm{id})}$, as well as the total density constraint, $\rho_{\mathrm{p}}^{(\mathrm{id})} + \rho_{\mathrm{at}}^{(\mathrm{id})} = \rho$. A straightforward calculation then provides

$$\rho_{\mathrm{p}}^{(\mathrm{id})} = \rho_{\mathrm{e}}^{(\mathrm{id})} = \rho^* \left(\sqrt{1 + 2\rho/\rho^*} - 1 \right) \tag{II.23}$$

and

$$\rho_{\mathrm{at}}^{(\mathrm{id})} = \rho^* \left(1 + \rho/\rho^* - \sqrt{1 + 2\rho/\rho^*} \right) \tag{II.24}$$

with temperature-dependent density

$$\rho^* = \frac{\exp(\beta E_{\mathrm{H}})}{2(2\pi\lambda_{\mathrm{pe}}^2)^{3/2}} \, . \tag{II.25}$$

According to those simple formulae, hydrogen becomes fully ionized for $\rho \ll \rho^*$, while it reduces to an atomic gas for $\rho \gg \rho^*$. This explains the behaviour of hydrogen inside the Sun, since the corresponding ratio ρ/ρ^* varies from 10^{-3} in the core to 10^7 in the photosphere.

4. Why atoms and not molecules?

In Earth atmosphere, hydrogen is a molecular gas and no atoms are present. This is oftenly explained by invoking that molecule H_2 is more stable than atom H,

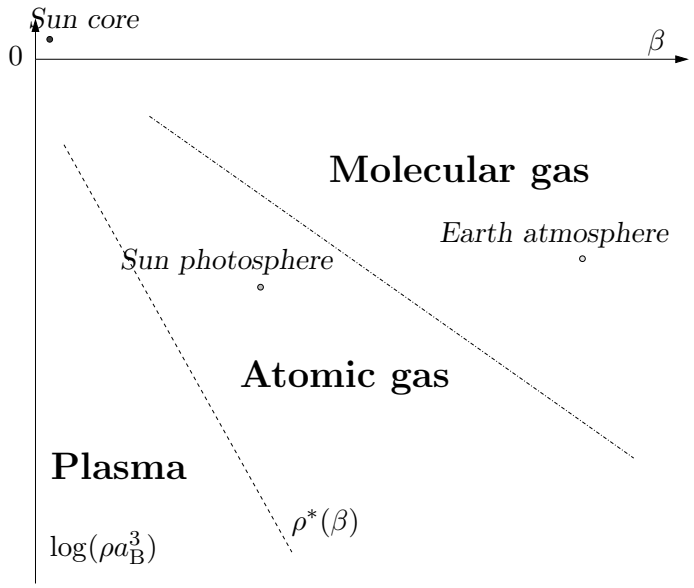

FIG. 3: Phase diagram of hydrogen at low densities. Regions where either ionized charges, atoms or molecules prevail, are separated by dashed ($\rho^*(\beta)$) and dash-dotted lines, in the vicinity of which the respective dissociation/recombination processes take place.

namely $E_{\mathrm{H}_2} < 2\ E_{\mathrm{H}}$, where E_{H_2} is the molecule groundstate energy. However, we stress that such an argument strictly applies at zero temperature, where only energy U^* intervene. At finite temperatures, $T > 0$, entropy S^* must be also considered in order to determine the chemical composition of the system. For a given number $N = N_p = N_e$ of protons and electrons enclosed in a box with volume Λ at a given temperature T, the entropy of the atomic gas is larger than that of its molecular counterpart, because the atom number $N_{\mathrm{H}} = N/2$ is twice the molecule number $N_{\mathrm{H}_2} = N/4$. Thus, in the minimization of the thermodynamic potential $(U^* - TS^*)$ at fixed T, Λ and N, entropy contribution favors the formation of atoms [78]. That effect becomes more important as T increases or $\rho = N/\Lambda$ decreases. In Earth atmosphere, temperature is rather low and density is rather high so only molecules are formed. In the Sun, temperature is sufficiently large and density sufficiently low so atoms prevail. The phase diagram of hydrogen at low densities is schematically drawn in Fig. 3.

5. What about the internal atomic partition function?

At finite temperatures, not only the atomic groundstate contributes to thermodynamic quantities, but also excited states. When T vanishes, an atom can be considered as frozen in its groundstate because of the finite gap between $E_{\rm H}$ and the first excited level $E_{\rm H}/4$. The corresponding contribution to equilibrium quantities merely involves Boltzmann factor $\exp(-\beta E_{\rm H})$. At finite temperatures, contributions of excited states must also be taken into account. For that purpose, it is natural to introduce the internal atomic partition function in the vacuum

$$Z_{\rm H}^{\rm (vac)} = 4 \sum_{n=1}^{\infty} \, n^2 \, \exp(-\beta E_{\rm H}/n^2) \; . \tag{II.26}$$

In that definition, factor 4 arises from proton and electron spins degeneracy, factor n^2 accounts for orbital degeneracy of the level n with energy $E_{\rm H}/n^2$, and summation extends over all boundstates up to $n = \infty$.

Obviously $Z_{\rm H}^{\rm (vac)}$ diverges because of the contributions of Rydberg states with $n \to \infty$. In the framework of the many-body problem, that divergency is usually expected to be cured thanks to screening effects, according to the following rough argument. At finite T and ρ, there is a finite amount of free charges, so the proton-electron potential inside an hydrogen atom decays faster than $1/r$ at distances r larger than screening length $\lambda_{\rm S}$. Thus, there is no accumulation of atomic boundstates near the continuum edge at $E = 0$, and all Rydberg states with n sufficiently large are suppressed. Since the spatial extension of such states is of order $n^2 a_{\rm B}$ with Bohr radius $a_{\rm B} = \hbar^2/(me^2)$, the infinite sum (II.26) has to be truncated up to $p_{\rm S} \sim (\lambda_{\rm S}/a_{\rm B})^{1/2}$. This provides a non-divergent atomic partition function,

$$Z_{\rm H}^{\rm (scr)} = 4 \sum_{n=1}^{p_{\rm S}} \, n^2 \, \exp(-\beta E_{\rm H}/n^2) \; , \tag{II.27}$$

which accounts for screening effects.

6. Are van der Waals interactions screened?

As guessed by van der Waals in his thesis, atoms or molecules attract themselves at large distances. For atoms with no permanent dipole, that interaction is due to

quantum fluctuations as first shown by London [25]. Let us sketch the corresponding calculation for two hydrogen atoms in their groundstate. Each atom i ($i = 1, 2$) is described by an Hamiltonian $H_{\rm at}^{(i)}$, and the full Hamiltonian of both atoms reads

$$H = H_{\rm at}^{(1)} + V_{\rm at,at} + H_{\rm at}^{(2)} \tag{II.28}$$

where $V_{\rm at,at}$ is the electrostatic interaction between the two atoms. For large separations R between such atoms, namely $R \gg a_{\rm B}$, that potential becomes dipolar because of atom charge neutrality, *i.e.*

$$V_{\rm at,at} \sim (\mathbf{p}_1 \cdot \boldsymbol{\nabla})\,(\mathbf{p}_2 \cdot \boldsymbol{\nabla})\,\frac{1}{R} \quad \text{when} \quad R \to \infty\,, \tag{II.29}$$

where $\mathbf{p}_i$ is the instantaneous electrical dipole carried by atom i. At such distances, when determining the groundstate energy of the whole two-atoms system, $V_{\rm at,at}$ can be treated as a small perturbation with respect to $H_{\rm at}^{(1)} + H_{\rm at}^{(2)}$. The first-order correction vanishes because the quantum average of $\mathbf{p}_i$ in the unperturbed groundstate is zero. The second-order correction can be reinterpreted as an atom-atom effective potential which reads [26]

$$U_{\rm vdW}(R) = -\frac{C_{\rm vdW}}{|E_{\rm H}|}\,\frac{e^4 a_{\rm B}^4}{R^6}\,. \tag{II.30}$$

In that expression, $C_{\rm vdW}$ is a pure numerical constant which is positive, so van der Waals potential $U_{\rm vdW}(R)$ is attractive. That potential appears to be generated by quantum fluctuations of the instantaneous $1/R^3$-dipolar interaction between two atoms : this explains the $1/R^6$-decay of $U_{\rm vdW}(R)$ at large distances, which merely follows by taking the square of $1/R^3$. Eventually, we check *a posteriori* that use of perturbation theory for deriving formula (II.30) is indeed justified if $R \gg a_{\rm B}$, since $|U_{\rm vdW}(R)|/|E_H|$ is proportional to $(a_{\rm B}/R)^6$.

Above derivation is performed for two isolated atoms at zero temperature in the vacuum. In the framework of the many-body system at finite T and ρ, besides the above difficulties in defining properly atoms, an interesting question concerns the effects of free charges on van der Waals interactions. Since the instantaneous atom-atom potential $V_{\rm at,at}$ is of purely Coulombic origin, screening mechanisms should modify $U_{\rm vdW}(R)$ at distances R larger than screening length $\lambda_{\rm S}$. A very crude and naive application of the classical recipe would lead to an exponential decay of the

effective atom-atom interactions. Nevertheless, and as it has been anticipated in the construction of the phenomenological Derjaguin-Landau-Verwey-Overbeek theory for mixtures of charged and neutral fluids [27–29], screening of van der Waals interactions should be less efficient than that prediction because of their underlying dynamical character. Hence, it is argued that the fast electronic motion embedded in quantum fluctuations of atom dipoles cannot be instantaneously followed by free charges because of inertia. According to that heuristic argument, it is oftenly assumed that $U_{\rm vdW}(R)$ is not screened at all. Notice that such argument is close to the one presented previously which suggests a breakdown of exponential screening in the quantum case.

III. SOME EXACT RESULTS WITHIN THE SCREENED CLUSTER REPRESENTATION

A. Fundamental issues and the hydrogen quantum plasma

In the previous introductory part of that lecture, various fundamental issues have been raised, namely

- *Nature of screening in quantum systems*
- *Introduction of recombined entities in the many-body problem*
- *Modification of van der Waals interactions due to free charges*

According to the preliminary analysis and discussions, it clearly appeared that a proper and reliable account of the relevant mechanisms requires the introduction of an elementary description of matter in terms of a quantum Coulomb system made with point nuclei and point electrons. For the sake of simplicity, and also because of its wide interest for both conceptual purposes and practical applications, here we will restrict ourselves to the hydrogen plasma viewed as a system of quantum point particles which are either protons or electrons, interacting via the instantaneous Coulomb potential. Protons and electrons have respective charges, masses, and

spins, $e_{\rm p} = e$ and $e_{\rm e} = -e$, $m_{\rm p}$ and $m_{\rm e}$, $\sigma_{\rm p} = \sigma_{\rm e} = 1/2$. In the present non-relativistic limit, the corresponding Hamiltonian for $N = N_{\rm p} + N_{\rm e}$ particles reads

$$H_{N_{\rm p},N_{\rm e}} = -\sum_{i=1}^{N} \frac{\hbar^2}{2m_{\alpha_i}} \Delta_i + \frac{1}{2} \sum_{i \neq j} e_{\alpha_i} e_{\alpha_j} v(|\mathbf{x}_i - \mathbf{x}_j|) \tag{III.1}$$

with $v(r) = 1/r$, $(\alpha_i = {\rm p}, {\rm e})$ the species of the ith particle, and Δ_i the Laplacian with respect to its position $\mathbf{x}_i$. In the following, we present several exact results for the equilibrium properties of that system, in relation with above fundamental issues.

First, in Section III B, we recall various rigorous results about the existence of the thermodynamic limit, as well as about the partially ionized atomic regime. Then, in Section III C, we introduce the path integral representation, in the simple case of a single particle submitted to an external potential for the sake of pedagogy. Application of that tool to the many-body quantum system leads to the introduction of an equivalent classical system made with extended objects called loops, which interact *via* a two-body potential equal to some average along their shapes of the genuine two-body particle interaction. The equilibrium quantities of the quantum plasma can then be represented by Mayer-like diagrammatical series in the loops world. In Section III D, we describe the resummation machinery which exactly transforms the sum of divergent Mayer graphs into a sum of convergent graphs with a similar structure, the so-called screened cluster representation (SCR). Long-range Coulomb divergences are removed *via* systematic chain resummations, which amount to introduce a screened effective potential between loops. Further reorganizations lead to the introduction of particle clusters with finite statistical weights, which include the contributions of familiar chemical species. Exact asymptotic expansions in the partially ionized atomic regime can be derived within that SCR, for both the equation of state and particle correlations, as decribed in Section III E. Eventually, we summarize in Section III F the main answers to the fundamental issues quoted above, which can be inferred from the present analysis of the hydrogen plasma.

B. Rigorous results

1. *Thermodynamic limit*

Let us consider the hydrogen plasma in the framework of the grand-canonical ensemble. The system is enclosed in a box with volume Λ, in contact with a thermostat at temperature T and a reservoir of particles that fixes the chemical potentials equal to $\mu_{\rm p}$ and $\mu_{\rm e}$ for protons and electrons respectively. The corresponding grand-partition function reads

$$\Xi_\Lambda = {\rm Tr}_\Lambda \exp\left(-\beta(H_{N_{\rm p},N_{\rm e}} - \mu_{\rm p}N_{\rm p} - \mu_{\rm e}N_{\rm e})\right) \ . \tag{III.2}$$

The trace ${\rm Tr}_\Lambda$ is taken over a complete basis of N-body wavefunctions, which are symmetrized according to Fermi statistics and satisfy Dirichlet boundary conditions at the surface of the box, while particle numbers $N_{\rm p}$ and $N_{\rm e}$ vary from 0 to ∞ [79].

The thermodynamic limit (TL) is defined by the limit $\Lambda \to \infty$ at fixed temperature and fixed chemical potentials. In that limit, Lieb and Lebowitz [30] proved the existence of a well-defined bulk equilibrium state with the right extensive properties expected from macroscopic thermodynamics. That state is overall neutral, namely the average particle densities $\rho_{{\rm p},\Lambda} = \langle N_{\rm p}\rangle/\Lambda$ and $\rho_{{\rm e},\Lambda} = \langle N_{\rm e}\rangle/\Lambda$ become identical in the TL,

$$\lim_{\rm TL} \rho_{{\rm p},\Lambda} = \lim_{\rm TL} \rho_{{\rm e},\Lambda} = \rho \ . \tag{III.3}$$

That common particle density depends only on temperature T and on the mean chemical potential

$$\mu = \frac{\mu_{\rm p} + \mu_{\rm e}}{2} \ , \tag{III.4}$$

while the difference $\nu = (\mu_{\rm e} - \mu_{\rm p})/2$ is not relevant. Pressure P defined by the standard formula

$$P = k_B T \lim_{\rm TL} \frac{\ln \Xi_\Lambda}{\Lambda} \tag{III.5}$$

is also a function of the two parameters T and μ, as well as all the other intensive thermodynamical quantities. Moreover, bulk properties no longer depend on the choosen boundary conditions, and all statistical ensembles become equivalent in the TL. In particular, grand-canonical expression (III.5) for pressure $P(T,\mu)$ does coincide with its canonical counterpart $P(T,\rho)$ evaluated at density $\rho = \rho(T,\mu)$.

Lieb and Lebowitz proof involves sophisticated mathematical analysis which will not be detailed here, of course! However, it is instructive to present the main ideas underlying the derivations. In fact, the central difficulties are related to the singular behaviours of the Coulomb potential at both short and large distances, as already quoted in Section II A. The short-distance collapse is avoided thanks to a combination of the Heisenberg uncertainty principle and of Fermi statistics. According to that principle, the $1/r$-singularity is smeared out, so the groundstate energy of N particles is finite, instead of $-\infty$ when opposite charges are present. Fermi statistics prevent the modulus of negative groundstate energies to grow faster than N. At a mathematical level, this is rephrased in the celebrated H-stability theorem [31],

$$H_{N_\mathrm{p},N_\mathrm{e}} > -B\,(N_\mathrm{p}+N_\mathrm{e}) \tag{III.6}$$

where B is a strictly positive constant. The large-distance explosion is prevented by screening mechanisms, the mathematical formulation of which is embedded in the cheese theorem. That theorem relies on a suitable partition of space in neutral spheres surrounding the charges, which applies for most probable configurations. Indeed, such configurations are overall neutral in the bulk while excess charges are repelled on the boundaries, as suggested by macroscopic electrostatics. The harmonicity of Coulomb potential then plays a crucial role, since according to Gauss theorem, two non-overlapping neutral spheres do not interact. This implies that dangerous long-range contributions do not intervene in the TL. Both cheese and H-stability theorems are the key ingredients of the proof.

2. Partially ionized atomic regime

In Section II D, we showed how, according to phenomenological Saha theory, a finite fraction of protons and electrons might recombine into hydrogen atoms, forming a partially ionized atomic gas. Also, we argued that such a regime should be attained when both temperature and density are sufficiently low so that individual atoms in their groundstate can form, namely $kT \ll |E_H|$ and $a \gg a_B$ with $a = (3/(4\pi\rho))^{1/3}$ the mean inter-particle distance.

The above Saha prediction has been rigorously proved within a suitable scaling

limit where both temperature and density vanish in a related way. That scaling limit is introduced in the framework of the grand-canonical ensemble : temperature T goes to zero while average chemical potential μ approaches the value E_H with a definite slope, according to parametrization [32]

$$\mu = E_{\rm H} + k_B T[\ln(\gamma) + \ln((m/M)^{3/4}/4)] \tag{III.7}$$

with fixed dimensionless parameter γ and $M = m_{\rm p} + m_{\rm e}$. Then density ρ indeed vanishes with T, and it behaves as

$$\rho = \rho^* \gamma (1 + \frac{\gamma}{2}) \left(1 + \mathcal{O}(e^{-c\beta})\right) \ , \tag{III.8}$$

with c a postive constant and temperature-dependent density ρ^* given by formula (II.25). The corresponding asymptotic behaviour of pressure P reads

$$\beta P = \rho^* \gamma (2 + \frac{\gamma}{2}) \left(1 + \mathcal{O}(e^{-c\beta})\right) \ . \tag{III.9}$$

Thus, if we discard the exponentially small corrections embedded in the $\mathcal{O}(e^{-c\beta})$-terms, the corresponding leading behaviours of density and pressure can be reinterpreted in terms of ideal densities of protons, electrons and atoms, identified to

$$\rho_{\rm p}^{\rm (id)} = \rho_{\rm e}^{\rm (id)} = \rho^* \gamma \tag{III.10}$$

and

$$\rho_{\rm at}^{\rm (id)} = \rho^* \frac{\gamma^2}{2} \ . \tag{III.11}$$

Such expressions do coincide with their Saha counterparts (II.23) and (II.24), as it can easily checked by eliminating γ in favor of ρ. Also, the pressure indeed reduces to that of an ideal mixture of protons, electrons and atoms, and it eventually reads

$$\beta P_{\rm Saha} = \rho^* \left(\rho/\rho^* + \sqrt{1 + 2\rho/\rho^*} - 1 \right) \ . \tag{III.12}$$

That rigorous derivation constitute another *tour de force* in mathematical physics, which has been implemented through successive works [32, 33] after the pionneering paper about the purely atomic limit by Fefferman [34]. Below, we sketch various estimations and arguments which provide a simple physical understanding of the result.

First, the above scaling limit defines the proper energy-entropy balance which ensures the emergence of the contributions of ionized protons, ionized electrons and hydrogen atoms in grand-partition function (III.2). That balance results from the competition between the fugacity factors $\exp(\beta\mu)$ which decay exponentially fast as $\exp(\beta E_{\rm H})$, and the groundstate Boltzmann factors which may explode exponentially fast. The relevant ideal contributions of ionized protons and ionized electrons are merely given by terms $(N_{\rm p}=1, N_{\rm e}=0)$ and $(N_{\rm p}=0, N_{\rm e}=1)$, and they are of order $\exp(\beta E_{\rm H})$. The corresponding atomic contribution, easily picked out in term $(N_{\rm p}=1, N_{\rm e}=1)$, is also of order $\exp(\beta E_{\rm H})$ since it involves the product of entropy factor $\exp(2\beta\mu)$ times the atomic Boltzmann factor $\exp(-\beta E_{\rm H})$. Thanks to remarkable inequalities [80] satisfied by the groundstate energies of Coulomb Hamiltonians $H_{N_{\rm p},N_{\rm e}}$ for $N_{\rm p}+N_{\rm e}\geq 3$, all the other contributions of more complex recombined entities decay faster than $\exp(\beta E_{\rm H})$. For instance, the molecular contribution embedded in term $(N_{\rm p}=2, N_{\rm e}=2)$ is of order $\exp(4\beta E_{\rm H})\exp(-\beta E_{\rm H_2})$, and it decays faster than $\exp(\beta E_{\rm H})$ by virtue of inequality [81]

$$3E_{\rm H} < E_{\rm H_2}\ . \tag{III.13}$$

Once, the contributions of molecules and other complex recombined entities have been discarded, it remains to estimate exchange and interaction contributions of ionized charges and atoms. In fact, since density vanishes exponentially fast, typically as $\exp(\beta E_{\rm H})$, the mean-interparticle distance $a=(3/(4\pi\rho))^{1/3}$ grows much faster, when $T\to 0$, than all thermal de Broglie wavelengths $\lambda_{\rm p}, \lambda_{\rm e}, \lambda_{\rm at}$ of ionized charges and atoms. Also, the average interactions between those entities, which are proportional to inverse powers of a, vanish exponentially fast when $T\to 0$, so they become negligible compared to thermal energy k_BT. Thus exchange and interaction contributions can be also dropped out in the scaling limit of interest. According to the previous simple estimations and rough arguments, it is not surprising that the system behaves as an ideal Maxwell-Boltzmann mixture of ionized protons, ionized electrons and atoms, in the considered scaling limit.

Let us define the so-called Saha regime by low but finite temperatures T, and very low but finite densities ρ of order $\exp(\beta E_{\rm H})$. According to the previous rigorous result, hydrogen should behave as a partially ionized atomic gas, weakly coupled

and weakly degenerate, including also small fractions of other complex entities, like molecules H_2 or ions H_2^+ and H^- for instance. As illustrated further, it is particularly interesting, at both practical and conceptual levels, to derive the corresponding corrections to the ideal terms obtained within Saha theory. For that purpose, it is convenient to combine the path integral representation to diagrammatical tools. Notice that the mathematical techniques involved in previous proof do not provide explicit expressions for the exponentially small corrections beyond ideal Saha formulas.

C. Path integral representation

1. Feynman-Kac formula

For the sake of pedagogy, we introduce the path integral representation in the simple case of a single particle with mass m submitted to a potential $V(\mathbf{r})$. Its Hamiltonian reads

$$H = -\frac{\hbar^2}{2m}\Delta + V(\mathbf{r}) \; . \tag{III.14}$$

The corresponding density matrix at a given temperature T, namely the matrix element of Gibbs operator $\exp(-\beta H)$, is exactly given by Feynman-Kac formula [35–38]

$$\langle \mathbf{r}_{\rm b}| \exp(-\beta H)|\mathbf{r}_{\rm a}\rangle = \frac{\exp[-(\mathbf{r}_{\rm b}-\mathbf{r}_{\rm a})^2/(2\lambda^2)]}{(2\pi\lambda^2)^{3/2}} \int \mathcal{D}(\boldsymbol{\xi}) \\ \times \exp[-\beta \int_0^1 {\rm d}s \; V\left((1-s)\;\mathbf{r}_{\rm a} + s\;\mathbf{r}_{\rm b} + \lambda\;\boldsymbol{\xi}(s)\right)] \; , \tag{III.15}$$

with thermal de Broglie wavelength $\lambda = (\beta\hbar^2/m)^{1/2}$. In the r.h.s. of (III.15), $\boldsymbol{\xi}(s)$ is a dimensionless Brownian bridge which starts from the origin at dimensionless time $s = 0$ and comes back at the origin at dimensionless time $s = 1$, *i.e.* $\boldsymbol{\xi}(0) = \boldsymbol{\xi}(1) = \mathbf{0}$. Functional measure $\mathcal{D}(\boldsymbol{\xi})$ is the normalized Gaussian Wiener measure which characterizes the Brownian process, and it is entirely defined by its covariance

$$\int \mathcal{D}(\boldsymbol{\xi})\; \xi_\mu(s)\; \xi_\nu(t) = \delta_{\mu\nu}\, \inf(s,t)\; (1 - \sup(s,t)) \; . \tag{III.16}$$

The corresponding functional integration is performed over all Brownian bridges $\boldsymbol{\xi}(s)$. Representation (III.15) is the proper mathematical formulation of genuine

Feynman's idea, which amounts to express the density matrix as a sum over all possible paths going from $\mathbf{r}_{\rm a}$ to $\mathbf{r}_{\rm b}$ in a time $\beta\hbar$, of weighting factors $\exp(-S/\hbar)$ where S is the classical action of a given path computed in potential $-V$. Here, such paths are parametrized according to

$$\boldsymbol{\omega}_{\rm ab}(s\beta\hbar) = (1-s)\ \mathbf{r}_{\rm a} + s\ \mathbf{r}_{\rm b} + \lambda\ \boldsymbol{\xi}(s)\ , \tag{III.17}$$

where $(1-s)\ \mathbf{r}_{\rm a} + s\ \mathbf{r}_{\rm b}$ describes the straight uniform path connecting $\mathbf{r}_{\rm a}$ to $\mathbf{r}_{\rm b}$ (see Fig 4.). Also, weighting factor $\exp(-S/\hbar)$ is splitted into the product of three terms. The first term, which arises from the kinetic energy of the straight uniform path, reduces to the Gaussian prefactor in front of the functional integral. The second term, associated with the kinetic contribution of the Brownian part of the path, is a Gaussian functional of $\boldsymbol{\xi}(s)$ embedded in Wiener measure $\mathcal{D}(\boldsymbol{\xi})$. The third and last term is rewritten as the Boltzmann-like factor associated with time average

$$\int_0^1 {\rm d}s\ V\left(\boldsymbol{\omega}_{\rm ab}(s\beta\hbar)\right) \tag{III.18}$$

of potential V along the considered path $\boldsymbol{\omega}_{\rm ab}$. We stress that, independently of the rather poetic introduction of path integrals by Feynman [39], representation (III.15) can be derived in a straightforward way by starting from the obvious identity $\exp(-\beta H) = [\exp(-\beta H/N)]^N$ combined with a suitable insertion of $(N-1)$ closure relations in position-space (see *e.g.* Ref. [6]). Feynman-Kac formula (III.15) then follows by taking the limit $N \to \infty$, as it has been proved for a wide class of potentials [35].

Feynman-Kac (FK) representation (III.15) perfectly illustrates the intrusion of dynamical features in equilibrium static quantities for quantum systems, which has been quoted in Section II C. Let us consider the diagonal density matrix $\langle \mathbf{r}_{\rm a}|\exp(-\beta H)|\mathbf{r}_{\rm a}\rangle$. Because of the non-commutativity of the kinetic and potential parts of H, that matrix element does not reduce to its classical counterpart

$$\frac{\exp(-\beta V(\mathbf{r}_{\rm a}))}{(2\pi\lambda^2)^{3/2}}\ , \tag{III.19}$$

so it is not entirely determined by $V(\mathbf{r}_{\rm a})$. In fact, according to formula (III.15) specified to $\mathbf{r}_{\rm b} = \mathbf{r}_{\rm a}$, $\langle \mathbf{r}_{\rm a}|\exp(-\beta H)|\mathbf{r}_{\rm a}\rangle$ now depends on the potential landscape in some neigbourhood of $\mathbf{r}_{\rm a}$ with size λ, which is explored in time-average (III.18) thanks to

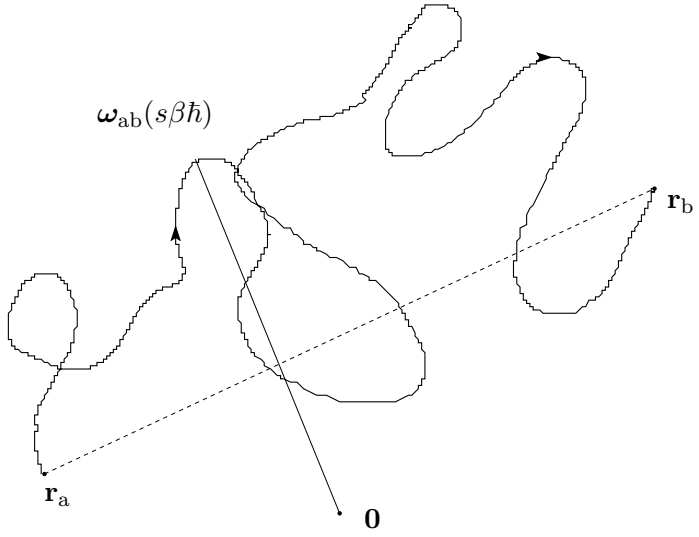

FIG. 4: A brownian path $\boldsymbol{\omega}_{\rm ab}(s\beta\hbar)$. The dashed straight line is the uniform path connecting $\mathbf{r}_{\rm a}$ to $\mathbf{r}_{\rm b}$.

Brownian motion. Therefore, $\langle \mathbf{r}_{\rm a}| \exp(-\beta H)|\mathbf{r}_{\rm a}\rangle$ appears to be indeed generated by a dynamical process. Not surprisingly, particle mass m controls the importance of the corresponding dynamical effects. In particular, in the limit of an infinitely heavy particle $m \to \infty$, $\lambda = (\beta\hbar^2/m)^{1/2}$ vanishes and $\langle \mathbf{r}_{\rm a}| \exp(-\beta H)|\mathbf{r}_{\rm a}\rangle$ obviously tends to its classical counterpart (III.19) : dynamical effects do not intervene anymore in the potential contribution which takes its purely static form [82]. Notice that the present dynamical considerations are the manifestation, in the framework of path integrals, of the Heisenberg uncertainty principle which prevents the particle to stay at $\mathbf{r}_{\rm a}$. Hence, Brownian paths can be interpreted as describing intrinsic quantum fluctuations of position.

Remarkably, FK representation (III.15) involves only classical objects and c-numbers, so the operatorial structure of quantum mechanics is, in some sense, erased. That feature turns out to be particularly useful in the framework of the many-body problem, as described further. However, the intrinsic complexity of quantum mechanics is now hidden in the functional integration over all Brownian bridges, which remains a formidable task. In fact, explicit calculations can be performed in a few number of cases, as reviewed in Ref. [38]. Also, aymptotic Wigner-Kirkwood expansions of $\langle \mathbf{r}_{\rm a}| \exp(-\beta H)|\mathbf{r}_{\rm a}\rangle$ around the classical formula (III.19), can be de-

rived for situations where λ becomes small compared to the characteristic length $[|\boldsymbol{\nabla} V(\mathbf{r}_{\rm a})|/|V(\mathbf{r}_{\rm a})|]^{-1}$ of variation of $V(\mathbf{r})$ in the neighbourhood of $\mathbf{r}_{\rm a}$. Such situations occur for very heavy particles or for high temperatures, and also at large distances for potentials which decay as power laws at infinity. In the opposite limit where λ diverges, direct estimations of FK functional integral become rather cumbersome. Notice that, if H has a single isolated boundstate with energy E_0 and wavefunction ψ_0, in the zero-temperature limit, the asymptotic behaviour of $\langle \mathbf{r}_{\rm a}| \exp(-\beta H)|\mathbf{r}_{\rm a}\rangle$ is merely extracted from its spectral representation, *i.e.*

$$\langle \mathbf{r}_{\rm a}| \exp(-\beta H)|\mathbf{r}_{\rm a}\rangle \sim |\psi_0(\mathbf{r}_{\rm a})|^2 \exp(-\beta E_0) \quad \text{when} \quad T \to 0 \; . \tag{III.20}$$

As argued in Ref. [43], the relevant paths which provide the low-temperature behaviour (III.20) occupy a small piece of the whole functional phase space, and they are quite different from the typical paths with divergent size λ. Consequently, an exact direct estimation of their contribution remains an open problem in general.

2. Gas of loops

Let us come back now to the hydrogen plasma in the framework of the grand-canonical ensemble described in Section III B. The trace in the grand-partition function (III.2) can be expressed in the basis of positions and spins, where a given state is the antisymmetrized Slater product of one-body states $|\mathbf{x}\, \sigma_\alpha^{(\rm z)}\rangle$. This provides a sum of diagonal and off-diagonal matrix elements of $\exp(-\beta H_{N_{\rm p},N_{\rm e}})$. An example of such matrix element with $(N_{\rm p}=3, N_{\rm e}=4)$ is

$$\langle \mathbf{R}_1\mathbf{R}_3\mathbf{R}_2\mathbf{r}_2\mathbf{r}_3\mathbf{r}_1\mathbf{r}_4| \exp(-\beta H_{3,4})|\mathbf{R}_1\mathbf{R}_2\mathbf{R}_3\mathbf{r}_1\mathbf{r}_2\mathbf{r}_3\mathbf{r}_4\rangle \; , \tag{III.21}$$

where the positions of two protons are exchanged, as well as those of three electrons. Contributions of spins are factored out in simple degeneracy factors because the Coulomb Hamiltonian $H_{N_{\rm p},N_{\rm e}}$ does not depend on the spins. For matrix element (III.21), that multipliyng degeneracy factor is 2^4, because the spin-states of the exchanged particles are necessarily identical.

The FK representation for each of the matrix elements of $\exp(-\beta H_{N_{\rm p},N_{\rm e}})$ takes a form similar to formula (III.15), with $N_{\rm p}$ protonic paths $\boldsymbol{\omega}^{(\rm p)}$ and $N_{\rm e}$ electronic

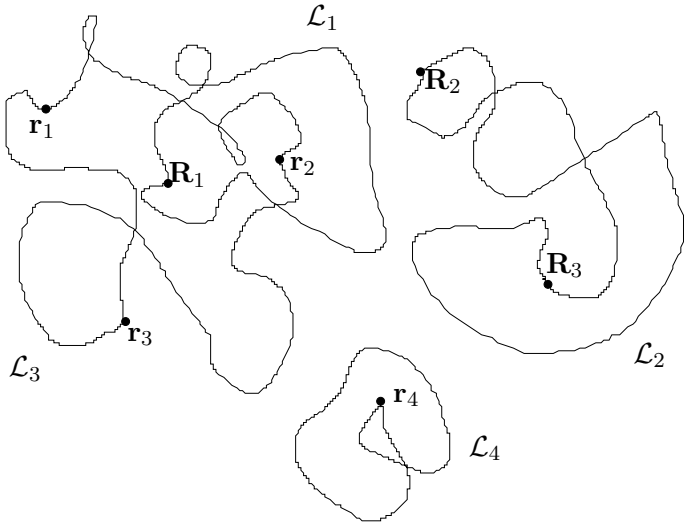

FIG. 5: A set of four loops constructed from matrix element (III.21).

paths $\boldsymbol{\omega}^{(\mathrm{e})}$, as well as a Boltzmann-like factor associated with the time average of the potential part $V_{N_\mathrm{p},N_\mathrm{e}}$ of $H_{N_\mathrm{p},N_\mathrm{e}}$. The paths associated with matrix element (III.21) are drawn in Fig. 5. We see that all those paths can be collected in loops. In fact, that property holds for any matrix element of $\exp(-\beta H_{N_\mathrm{p},N_\mathrm{e}})$, because any permutation can always be decomposed as a product of cyclic permutations. A loop $\mathcal{L}$ is constructed by collecting q paths associated with q particles exchanged in a cyclic permutation. Accordingly, $\mathcal{L}$ is characterized by its position $\mathbf{X}$, which can be arbitrarily chosen among the extremities of paths $\boldsymbol{\omega}$, and several internal degrees of freedom which are particle species ($\alpha = \mathrm{p}, \mathrm{e}$), number q of exchanged particles, and shape $\lambda_\alpha\, \boldsymbol{\eta}$ obtained as the union of the q paths $\boldsymbol{\omega}$. It turns out that $\boldsymbol{\eta}(s)$ is itself a Brownian bridge with flight time q, *i.e.* $\boldsymbol{\eta}(0) = \boldsymbol{\eta}(q) = \mathbf{0}$, distributed with the corresponding Wiener measure $\mathcal{D}(\boldsymbol{\eta})$.

In the FK representation, the time-average of potential $V_{N_\mathrm{p},N_\mathrm{e}}$ can be obviously rewritten as a sum of two-body interactions $\mathcal{V}$ between loops, plus a sum of loop self-energies $\mathcal{U}$, namely

$$\frac{1}{2}\sum_{i\neq j}\mathcal{V}(\mathcal{L}_i,\mathcal{L}_j)+\sum_i \mathcal{U}(\mathcal{L}_i)\;, \tag{III.22}$$

where loops associated with the considered matrix element are labelled as $\mathcal{L}_i$ with index i running from 1 to their total number N. For instance, four loops can be identified in the FK representation of matrix element (III.21). Two-body potential

$\mathcal{V}(\mathcal{L}_i, \mathcal{L}_j)$ between loops $\mathcal{L}_i$ and $\mathcal{L}_j$ reduces to a time-average along their respective shapes of the genuine two-body particle interaction $v(|\mathbf{X}_i+\lambda_{\alpha_i}\boldsymbol{\eta}_i(s)-\mathbf{X}_j-\lambda_{\alpha_j}\boldsymbol{\eta}_j(t)|)$ evaluated at times which differ by an integer value. Self-energy $\mathcal{U}(\mathcal{L}_i)$ for loop $\mathcal{L}_i$ is given by a similar average along its own shape of $v(|\lambda_{\alpha_i}\boldsymbol{\eta}_i(s) - \lambda_{\alpha_i}\boldsymbol{\eta}_i(t)|)$ evaluated at times which differ by a non-zero integer value, with a prefactor $1/2$ which avoids double counting of genuine interactions between two exchanged particles.

At this stage, grand-partition function (III.2) is rewritten as a sum of Boltzmann-like factors associated with energies (III.22) multiplied by combinatorial factors and particle fugacities $z_\alpha/(2\pi\lambda_\alpha^2)^{3/2}$ with $z_\alpha = \exp(\beta\mu_\alpha)$, which have to be integrated over positions and shapes of the involved loops. It turns out that the whole sum can be rewritten as the grand-partition function of a classical gas of undistinguishable loops with suitable activities $z(\mathcal{L})$, namely

$$\Xi_\Lambda = \Xi_\Lambda^{(\mathrm{loop})} = \sum_{N=0}^{\infty} \frac{1}{N!} \int \prod_{i=1}^{N} \mathrm{d}\mathcal{L}_i \; z(\mathcal{L}_i) \prod_{i<j} \exp(-\beta \mathcal{V}(\mathcal{L}_i, \mathcal{L}_j)) \; . \tag{III.23}$$

Phase space measure $\mathrm{d}\mathcal{L}$ in the world of loops, involves discrete summations over species index α and exchanged-particle number q, spatial integration over position $\mathbf{X}$ inside Λ, and functional integration over shapes $\boldsymbol{\eta}$ with Wiener measure $\mathcal{D}(\boldsymbol{\eta})$ restricted to shapes such that $\mathbf{X} + \lambda_\alpha\boldsymbol{\eta}(s)$ remains inside Λ. Loop fugacity reads

$$z(\mathcal{L}) = (-1)^{q-1} \, \frac{2 z_\alpha^q}{q(2\pi q \lambda_\alpha^2)^{3/2}} \, \exp(-\beta \mathcal{U}(\mathcal{L})) \; , \tag{III.24}$$

the structure of which is easily intepreted as follows. Factor $(-1)^{q-1}$ is the signature of a cyclic permutation of q objects. In front of the obvious particle-activity contribution z_α^q, factor 2 is the number of configurations of exchanged-particles spins which are all identical. Factor q in front of $(2\pi q\lambda_\alpha^2)^{3/2}$ is related to the q possible choices of position $\mathbf{X}$ among that of the q exchanged particles. The other factor q in front of λ_α^2, arises from the absorption of the remaining $(q-1)$ integrations over particle positions together with the q functional integrations over Brownian bridges into the single measure $\mathcal{D}(\boldsymbol{\eta})$. Notice that $q\lambda_\alpha^2$ is nothing but the square of de Broglie wavelength for inverse temperature $q\beta$.

We stress that identity (III.23) proceeds from remarkable combinatorial properties. For instance, in $\Xi_\Lambda^{(\mathrm{loop})}$, there are various contributions in term $N = 4$,

which are identical to that of matrix element (III.21) in the Slater expansion of Ξ_Λ. Such contributions arise from the explicitation of the 4 phase-space measures $\mathrm{d}\mathcal{L}_i$ ($i = 1, 2, 3, 4$) where 2 protonic loops and 2 electronic loops, carrying respectively 2 or 1 protons and 3 or 1 electrons, have to be chosen among 4 labelled loops. Also, there are several matrix elements in the Slater expansion of Ξ_Λ, involving 3 protons and 4 electrons, which provide identical contributions to that of matrix element (III.21). Thanks to a rather fortunate arrangment between both counting factors, the full respective contributions in both $\Xi_\Lambda^{(\mathrm{loop})}$ and Ξ_Λ are indeed identical! According to those considerations, and also because of its synthetical form, identity (III.23) is oftenly called the magic formula.

Historically, Ginibre [44] was the first to introduce the notion of loops when studying the convergence of Mayer series for quantum gases with short-range forces. However, he did not write explicitely formula (III.23), which has been derived later by Cornu [45]. Recently, Martin [46] proposed an elegant and shorter derivation of that formula. Notice that identity (III.23) is valid for any kind of two-body interactions, and an arbitrary number of species with Fermi or Bose statistics. For a bosonic species, factor $(-1)^{q-1}$ is merely replaced by 1 in loop fugacity (III.24), while all the other factors are unchanged. Magic formula (III.23) has been applied to a Bose gas with short-range interactions for studying Bose-Einstein condensation [47].

Of course, and as quoted in the simple case of a single particle in an external potential, the intrinsic difficulty of quantum mechanics is now hidden in the functional integrations over loop shapes, so an exact calculation of loop grand-partition function remains far beyond human abilities...Nevertheless, magic formula (III.23) is quite useful because standard tools of classical statistical mechanics can be applied, as well as various transformations relying on simple properties of classical Boltzmann factors.

D. Screened cluster representation

From now on, we assume that the thermodynamic limit has been taken once for all. Since, according to Lieb and Lebowitz theorems, boundary effects do not

intervene anymore in the TL, we proceed to formal calculations in the infinite system where some quantities are infinite. Nonetheless, after suitable resummations and reorganizations, such divergences are removed, and it is quite reasonable to believe that the final results are indeed relevant, as far as they are finite, and they do describe the considered bulk quantities. That strategy is adopted for the calculation of particle densities and particle correlations. Also we work in the world of loops. According to magic formula (III.23), those particle quantities are merely related to their loop counterparts. For instance, proton density $\rho_{\rm p}$ is given in terms of loop density $\rho(\mathcal{L}_{\rm a})$ by

$$\rho_{\rm p} = \sum_{q_{\rm a}=1}^{\infty} \int \mathcal{D}(\boldsymbol{\eta}_{\rm a})\; q_{\rm a}\; \rho(\mathcal{L}_{\rm a})\;, \tag{III.25}$$

where loop species index is $\alpha_{\rm a} = {\rm p}$.

1. *Mayer graphs*

The structure of loop grand-partition (III.23) is identical to that of an ordinary classical system made of point particles with two-body interactions. Therefore, equilibrium quantities of loops can be represented by Mayer-like diagrammatical series, where points are replaced by loops. This provides Mayer series for particle quantities, like proton density $\rho_{\rm p}$ which reads

$$\rho_{\rm p} = \sum_{\mathcal{G}} \frac{1}{S(\mathcal{G})} \sum_{q_{\rm a}=1}^{\infty} \int \mathcal{D}(\boldsymbol{\eta}_{\rm a})\; q_{\rm a}\; z(\mathcal{L}_{\rm a}) \int \prod_{i=1}^{n} {\rm d}\mathcal{L}_i\; z(\mathcal{L}_i) \left[\prod f\right]_{\mathcal{G}}\;. \tag{III.26}$$

Each graph $\mathcal{G}$ is constructed according to the standard Mayer rules [48, 49]. It is made with $(n+1)$ loops $\mathcal{L}_i$, $i = 0, ..., n$ and $\mathcal{L}_0 = \mathcal{L}_{\rm a}$. Two loops i and j are connected at most by a single bond

$$f_{ij} = \exp(-\beta \mathcal{V}(\mathcal{L}_i, \mathcal{L}_j)) - 1\;, \tag{III.27}$$

and $[\prod f]_{\mathcal{G}}$ denotes the product of such bonds. Also, graph $\mathcal{G}$ is simply connected, namely it cannot be separated into two parts which are not connected by at least one bond f. Symmetry factor $S(\mathcal{G})$ is the number of permutations of black loops $\mathcal{L}_i$ with $i \geq 1$, which leave $\prod_{\mathcal{G}} f$ unchanged. Each loop is weighted by its fugacity $z(\mathcal{L}_i)$. The contribution of graph $\mathcal{G}$ is obtained by integrating over all degrees of freedom

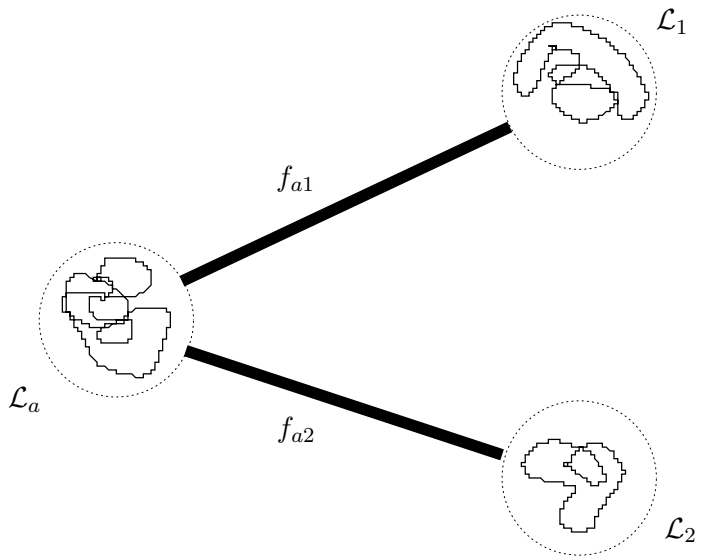

FIG. 6: A graph $\mathcal{G}$ made with root loop $\mathcal{L}_a$ and two field loops $\mathcal{L}_1$ and $\mathcal{L}_2$.

of black loops embedded in measure $\mathrm{d}\mathcal{L}_i$, while the position and species index of root loop $\mathcal{L}_\mathrm{a}$ are fixed and only its shape and particle number are integrated over. Eventually, $\sum_{\mathcal{G}}$ is performed over all topologically different unlabelled graphs $\mathcal{G}$. An example of graph $\mathcal{G}$ is shown in Fig. 6, while its contribution reads

$$\frac{1}{2}\sum_{q_\mathrm{a}=1}^{\infty}\int \mathcal{D}(\boldsymbol{\eta}_\mathrm{a})\; q_\mathrm{a}\; z(\mathcal{L}_\mathrm{a}) \int \mathrm{d}\mathcal{L}_1 \mathrm{d}\mathcal{L}_2\; z(\mathcal{L}_1) z(\mathcal{L}_2) f_{\mathrm{a}1} f_{\mathrm{a}2}\;. \tag{III.28}$$

The loop-loop interaction is long ranged, like the genuine Coulomb potential itself, as illustrated by the large distance behaviour

$$\mathcal{V}(\mathcal{L}_i,\mathcal{L}_j) \sim \frac{q_i e_{\alpha_i} q_j e_{\alpha_j}}{|\mathbf{X}_i-\mathbf{X}_j|} \quad \text{when} \quad |\mathbf{X}_i-\mathbf{X}_j|\to\infty\;. \tag{III.29}$$

Indeed, at large distances, loops can be shrinked to point charges, and further corrections to the monopolar form (III.29) can be expanded in multipolar power series of $\lambda_{\alpha_i}/|\mathbf{X}_i-\mathbf{X}_j|$ and $\lambda_{\alpha_j}/|\mathbf{X}_i-\mathbf{X}_j|$. Like in the case of purely Coulombic interactions, the long-range nature of $\mathcal{V}(\mathcal{L}_i,\mathcal{L}_j)$ induces divergences as explained in Section II A for purely Coulombic interactions. Here, in Mayer series (III.26), such divergences pollute every graph because Mayer bonds behave as $-\beta\mathcal{V}(\mathcal{L}_i,\mathcal{L}_j)$ at large distances.

In addition to previous long-range pollution, another drawback of Mayer series relies on the difficulty to identify immediately the contributions of a given chemical

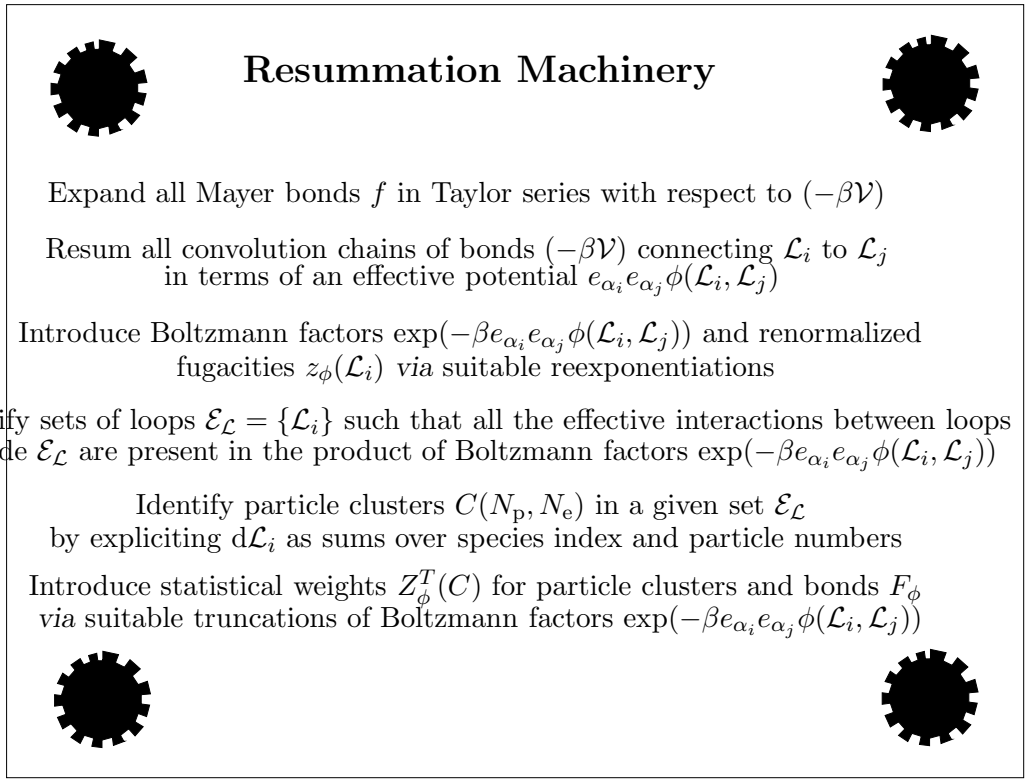

FIG. 7: Main steps of the resummatiom machinery.

species. For instance, if we are interested in contribution of ion H_2^+ to series (III.26), we can pick out in contribution (III.28) of graph drawn in Fig. 6, the term ($q_\mathrm{a}=1,\alpha_\mathrm{a}=\mathrm{p}\ ;q_1=1,\alpha_1=\mathrm{p}\ ;q_2=1,\alpha_2=\mathrm{e}$), which involves 2 protons and 1 electron. However, because of the absence of bond f_{12} in that graph, a proton-electron interaction is missing. The full interaction between the two protons and the single electron is recovered by summing contributions from all graphs $\mathcal{G}$ made with three loops.

2. Resummation machinery

The resummation machinery amounts to perform an exact transformation of the whole series (III.26), which takes care of drawbacks of Mayer grahs quoted above. The main steps are sketched in Fig. 7. Of course, all the transformations involve tricky counting calculations based on combinatorial identities, which are detailed in Ref. [50]. The final result can be expressed as the Screened Cluster Representation

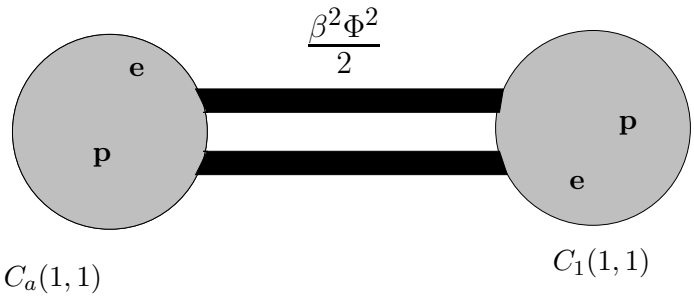

FIG. 8: A graph G made with root cluster $C_a(1,1)$ and one field cluster $C_1(1,1)$. Each cluster contains one proton and one electron denoted by symbols **p** and **e** respectively.

(SCR),

$$\rho_{\rm p} = \sum_G \frac{1}{S(G)} \int {\rm d}C_{\rm a}\; q_{\rm a}\; Z_\phi^T(C_{\rm a}) \int \prod_{i=1}^{n} {\rm d}C_i\; Z_\phi^T(C_i) \left[\prod \mathcal{F}_\phi\right]_G \;, \tag{III.30}$$

where graphs G have the same topological structure as usual Mayer graphs. Now, ordinary points are replaced by particle clusters C_i, weighted by factors $Z_\phi^T(C_i)$. Two clusters are connected by at most one bond F_ϕ which can be either $-\beta\Phi$, $\beta^2\Phi^2/2!$ or $-\beta^3\Phi^3/3!$ with Φ the total effective potential between both clusters. Graphs G are simply connected, and symmetry factor $S(G)$ is computed as usual. Phase-space measure ${\rm d}C_i$ reduces to integrations over positions and shapes of loops belonging to set $\mathcal{E}_\mathcal{L}$ associated with cluster C_i, whereas in ${\rm d}C_{\rm a}$ position of root proton is not integrated over. Eventually, $\sum_G$ is performed over all topologically different graphs with some simple restrictions, in part avoiding double-counting of genuine particle interactions [50]. In Fig. 8, we give an example of graph G, made with two clusters $C_{\rm a} = C_{\rm a}(1,1)$ and $C_1 = C_1(1,1)$. Its contribution reads

$$\int {\rm d}C_{\rm a}\; Z_\phi^T(C_{\rm a}) \int {\rm d}C_1\; Z_\phi^T(C_1)\; \frac{\beta^2\Phi^2(C_{\rm a}, C_1)}{2} \;, \tag{III.31}$$

since $S(G) = 1$ and $q_{\rm a} = 1$. Notice that part of graph $\mathcal{G}$ shown in Fig. 6 contributes to previous graph G under the action of the resummation machinery.

Remarkably, not only the genuine structure of Mayer graphs is conserved through the resummation machinery, but both statistical weights $Z_\phi^T(C)$ and bonds F_ϕ depend on the sole effective potential ϕ. Thanks to the sufficient fast decay of ϕ, all large-distances divergences are removed in every graph G, which does provide a finite contribution. The presence of complete interactions inside a given cluster

$C(N_{\rm p},N_{\rm e})$ ensures that chemical species made with $N_{\rm p}$ protons and $N_{\rm e}$ electrons do emerge at low densities. Both features are detailed below. Notice that the physical ideas underlying the SCR, are close to those involved in the construction of the so-called ACTEX approach by Rogers [51]. Also, contrarily to Feynman graphs involved in standard many-body perturbation theory [20], graphs G in SCR account for non-perturbative effects in the Coulomb potential which are essential for a proper description of recombination.

3. Screened effective potential

Effective potential $e_{\alpha_{\rm a}}e_{\alpha_{\rm b}}\phi(\mathcal{L}_{\rm a},\mathcal{L}_{\rm b})$ is defined by the sum of all convolution chains of bonds $(-\beta\mathcal{V})$ connecting $\mathcal{L}_{\rm a}$ to $\mathcal{L}_{\rm b}$, namely

$$e_{\alpha_{\rm a}}e_{\alpha_{\rm b}}\phi(\mathcal{L}_{\rm a},\mathcal{L}_{\rm b})=\mathcal{V}(\mathcal{L}_{\rm a},\mathcal{L}_{\rm b})+\sum_{n=1}^{\infty}(-1)^n\beta^n\int\prod_{i=1}^{n}{\rm d}\mathcal{L}_i\;z(\mathcal{L}_i)\;\mathcal{V}(\mathcal{L}_{i-1},\mathcal{L}_i)\;\mathcal{V}(\mathcal{L}_n,\mathcal{L}_{\rm b})\;, \tag{III.32}$$

with $\mathcal{L}_0=\mathcal{L}_{\rm a}$. That potential accounts for collective effects, because it involves contributions of an infinite number of loops. Interestingly, chain sum (III.32) can be reinterpreted as the complete perturbative expansion of the solution of integral equation

$$e_{\alpha_{\rm a}}e_{\alpha_{\rm b}}\phi(\mathcal{L}_{\rm a},\mathcal{L}_{\rm b})=\mathcal{V}(\mathcal{L}_{\rm a},\mathcal{L}_{\rm b})-\beta\int{\rm d}\mathcal{L}\;z(\mathcal{L})\;e_{\alpha_{\rm a}}e_{\alpha}\phi(\mathcal{L}_{\rm a},\mathcal{L})\mathcal{V}(\mathcal{L},\mathcal{L}_{\rm b})\;. \tag{III.33}$$

Therefore, $e_{\alpha_{\rm a}}e_{\alpha_{\rm b}}\phi(\mathcal{L}_{\rm a},\mathcal{L}_{\rm b})$ is the total potential acting on loop $\mathcal{L}_{\rm b}$, created by loop $\mathcal{L}_{\rm a}$ plus a cloud of loops $\mathcal{L}$ distributed with density $-\beta z(\mathcal{L})\;e_{\alpha_{\rm a}}e_{\alpha}\phi(\mathcal{L}_{\rm a},\mathcal{L})$. Its physical content is then quite similar to that of the Debye potential introduced in Section II B. In the classical limit $\hbar\to 0$, loops shrink to point charges so equation (III.33) is nothing but the integral version of linearized Poisson-Boltzmann equation (II.9) with $\epsilon_{\rm w}=1$. Thus, the effective potential $e_{\alpha_{\rm a}}e_{\alpha_{\rm b}}\phi(\mathcal{L}_{\rm a},\mathcal{L}_{\rm b})$ can be viewed as the quantum analogue of the Debye potential [52].

Similarly to what happens in the classical case, collective effects embedded in the effective potential are expected to screen the bare loop-loop interaction. In fact, the static part $q_{\rm a}e_{\alpha_{\rm a}}q_{\rm b}e_{\alpha_{\rm b}}/|\mathbf{X}_{\rm a}-\mathbf{X}_{\rm b}|$ of $\mathcal{V}(\mathcal{L}_{\rm a},\mathcal{L}_{\rm b})$, which does not depend on loop shapes, is exponentially screened [83]. On the contrary, the multipolar parts of $\mathcal{V}(\mathcal{L}_{\rm a},\mathcal{L}_{\rm b})$

which depend on loop shapes, are not exponentially screened. The resulting effective potential decays only as a dipolar interaction at large distances, namely [52]

$$\phi(\mathcal{L}_{\rm a},\mathcal{L}_{\rm b}) \sim \frac{\mathcal{A}_{\alpha_{\rm a}\alpha_{\rm b}}(\boldsymbol{\eta}_{\rm a},\boldsymbol{\eta}_{\rm b})}{|\mathbf{X}_{\rm a}-\mathbf{X}_{\rm b}|^3} \quad \text{when} \quad |\mathbf{X}_{\rm a}-\mathbf{X}_{\rm b}|\to\infty\ , \tag{III.34}$$

where $\mathcal{A}_{\alpha_{\rm a}\alpha_{\rm b}}(\boldsymbol{\eta}_{\rm a},\boldsymbol{\eta}_{\rm b})$ is an amplitude which depends only on loop species and shapes. Consequently, bonds $F_\phi = -\beta\Phi$ are at the border line for integrability at large distances. However, if loop shapes are first integrated over, all dangerous $1/R^3$-terms vanish. Thus, within that prescription for the order of integrations involved in measures $\mathrm{d}C_i$, each graph G in SCR (III.30) indeed provides a finite contribution.

The slow algebraic decay of ϕ can be understood as follows. As mentionned in Section III C, paths defining loop shapes account for intrinsic quantum fluctuations of particle positions. Such fluctuations, which are dynamical in origin, generate $1/R^3$-dipolar interactions. In agreement with heuristic findings argued in Section II C, such dynamical interactions cannot be perfectly screened trough collective effects, so it remains a $1/R^3$-tail in the large-distance behaviour of ϕ.

4. Emergence of chemical species

As quoted in Section II D, familiar chemical species may emerge, strictly speaking, in a zero-density limit only. Not surprisingly, in such a limit, effective potential $e_{\alpha_{\rm a}}e_{\alpha_{\rm b}}\phi(\mathcal{L}_{\rm a},\mathcal{L}_{\rm b})$ reduces to the bare loop-loop interaction $\mathcal{V}(\mathcal{L}_{\rm a},\mathcal{L}_{\rm b})$ as shown in Ref. [52]. Let us consider the contribution of the simple graph G made with the single root cluster $C_{\rm a}(N_{\rm p},N_{\rm e})$. Functional integrations over loop shapes of products of Boltzmann factors $\exp(-\beta\mathcal{V}(\mathcal{L}_i,\mathcal{L}_j))$ embedded in $Z_\phi^T(C_{\rm a})$, can be expressed in terms of matrix elements of Gibbs operators associated with Coulomb Hamiltonians, by applying backwards FK formula. Then, the contribution of the considered graph G is proportional to

$$Z(N_{\rm p},N_{\rm e}) = \frac{(2\pi\lambda^2_{N_{\rm p}N_{\rm e}})^{3/2}}{\Lambda}\mathrm{Tr}\left[\exp(-\beta H_{N_{\rm p},N_{\rm e}})-...\right] \tag{III.35}$$

with $\lambda^2_{N_{\rm p}N_{\rm e}} = \beta\hbar^2/(N_{\rm p}m_{\rm p}+N_{\rm e}m_{\rm e})$. Terms ... left over in the r.h.s. of definition (III.35) indicate a suitable truncation of Gibbs operator $\exp(-\beta H_{N_{\rm p},N_{\rm e}})$, which ensures the finiteness of the trace. Thus, we see that SCR leads to a natural definition

of the partition function $Z(N_{\rm p}, N_{\rm e})$ for $N_{\rm p}$ protons and $N_{\rm e}$ electrons in the vacuum. That partition function includes the contribution of possible recombined species in their groundstate, as well as those of thermal excitations.

At finite densities, $Z_\phi^T(C_{\rm a})$ accounts for many-body effects on cluster $C_{\rm a}$, like the broadening and shift of energy levels of recombined species made with $N_{\rm p}$ protons and $N_{\rm e}$ electrons. Also, graphs G with several clusters describe interactions between such clusters which are screened by ionized charges. For instance graph shown in Fig. 8, involves contributions from interactions between two atoms. In fact, all phenomena at work can be identified in specific graphs, as argued in Ref. [50].

E. Asymptotic expansions in the Saha regime

1. *Equation of state*

Now, we consider again the Saha regime, where hydrogen behaves as a partially ionized atomic gas. We start with a grand-canonical description, where the given thermodynamic parameters are μ and T, and common particle density $\rho = \rho_{\rm p} = \rho_{\rm e}$ is a function $\rho(\mu, T)$. Making the variable change $(\mu, T) \to (\gamma, T)$ defined through parametrization (III.7), we see that density can also be viewed as a function of γ and T. Then, we proceed to the expansion of $\rho(\gamma, T)/\rho^*$ when $T \to 0$ at fixed γ, by investigating the corresponding behaviour of graphs G in SCR (III.30). Roughly speaking, that behaviour results from the competition between three kind of contributions, which vanish or explode exponentially fast when $T \to 0$, namely

(i) $\gamma^N \exp(\beta N E_{\rm H})$ with $N = N_{\rm p} + N_{\rm e}$ arising from entropy factor $\exp(\beta\mu N)$ in $Z_\phi^T(C)$

(ii) $\exp(-\beta E^{(0)}_{N_{\rm p},N_{\rm e}})$ arising from a recombined entity with groundstate energy $E^{(0)}_{N_{\rm p},N_{\rm e}}$ in $Z_\phi^T(C)$

(iii) $\gamma^{p/2} \exp(\beta p E_{\rm H}/2)$ with p relative integer, arising from interactions screened over Debye length $\lambda_{\rm D} = (4\pi\beta e^2(\rho_{\rm p}^{\rm (id)} + \rho_{\rm e}^{\rm (id)}))^{-1/2}$ with $\rho_{\rm p}^{\rm (id)} = \rho_{\rm e}^{\rm (id)} = \rho^*\gamma$ in bonds $\mathcal{F}_\phi$ between charged clusters [84]

Previous analysis provides the Scaled Low Temperature expansion of $\rho(\gamma,T)/\rho^*$, where leading terms

$$\gamma+\frac{\gamma^2}{2} \tag{III.36}$$

are indeed those predicted by Saha theory. Each correction reduces to some power of γ multiplied by a temperature-dependent function which decays exponentially fast when $T\to 0$, in agreement with the rigorous behaviour (III.8) presented in Section III B.

The SLT expansion of $\beta P/\rho^*$ is readily obtained from that of $\rho(\gamma,T)/\rho^*$, by integrating identity

$$\frac{\partial\beta P}{\partial\gamma}(\beta,\gamma)=\frac{2\rho}{\gamma} \tag{III.37}$$

whichs follows from the standard thermodynamical relation between ρ, P and μ. A further elimination of γ between both SLT expansions of $\beta P(\gamma,T)/\rho^*$ and $\rho(\gamma,T)/\rho^*$ provides the SLT expansion of the equation of state, *i.e.* the asymptotic expansion of pressure in units of $\rho^* k_{\rm B}T$ when $T\to 0$ at fixed ratio ρ/ρ^*,

$$\beta P/\rho^*=\beta P_{\rm Saha}/\rho^*+\sum_{k=1}^{\infty} b_k(\rho/\rho^*)\alpha_k(\beta)\ . \tag{III.38}$$

The leading term is indeed given by Saha formula (III.12). Coefficients $b_k(\rho/\rho^*)$ are algebraic functions of ratio ρ/ρ^*, while temperature-dependent functions $\alpha_k(\beta)$ decay exponentially fast when T vanishes, $\alpha_k(\beta)\sim\exp(-\beta\delta_k)$ except for possible multiplicative powers of β. Expansion (III.38) is ordered with respect to increasing decay rates, $0<\delta_1<\delta_2<....$ The first five corrections have been computed in Ref. [53] (see Ref. [54] for a pedagogical presentation of the calculations). In the following table, we summarize their physical content, as well as the expressions and values of the corresponding decay rates which are merely obtained by taking the products of above exponential factors (i), (ii) and (iii).

Correction (k)	Physical content	δ_k (in eV)
1	plasma polarization around ionized charges	$\lvert E_{\rm H}\rvert/2\simeq 6.8$
2	formation of molecules, atom-atom interactions	$\lvert 3E_{\rm H}-E_{\rm H_2}\rvert\simeq 9.1$
3	atomic excitations, charge-charge interactions	$3\lvert E_{\rm H}\rvert/4\simeq 10.2$
4	formation of ions, atom-charge interactions	$\lvert 2E_{\rm H}-E_{\rm H_2^+}\rvert\simeq 11.0$
5	fluctuations of plasma polarization	$\lvert E_{\rm H}\rvert\simeq 13.6$

Remarkably, all non-ideal corrections to Saha equation of state evocated in Section III B are properly identified and ordered in exact SLT expansion (III.38). Contributions of usual chemical species do emerge in the present double low-temperature and low-density limit, in agreement with heuristic findings presented in Section II D. Their relative importance, determined by the ordering of decay rates δ_k, results from subtle inequalities between groundstate energies $E^{(0)}_{N_\mathrm{p},N_\mathrm{e}}$ and E_H in the vacuum. For instance, formation of molecules H_2 dominate that of ions H_2^+ or H^-, while contributions of more complex entitites, like H_2^-, H_3^+ or H_3, decay exponentially faster than $\exp(-\beta|E_\mathrm{H}|)$ as detailed in Ref. [53]. Thermal excitations of atoms, molecules and ions are accounted for in functions $\alpha_k(\beta)$ *via* the corresponding cluster partition functions $Z(1,1)$, $Z(2,2)$, $Z(2,1)$ and $Z(1,2)$. However, we stress that such contributions of recombined entities are entangled to that of their dissociation products. For instance, in $Z(1,1)$, contributions from excited atomic states cannot be separated from that of ionized protons and ionized electrons. Also, those cluster partition functions, built with bare Coulomb Hamiltonians, are indeed finite thanks to the substraction of non-integrable long-range parts, which are ultimately screened by ionized charges. Thus, only the full contribution of those species partition functions and of their screened long-range parts, makes physical sense. For instance, term $k = 3$ involves both contributions of $Z(1,1)$ and of screened proton-electron interactions. In that context, the extraction from $\alpha_3(\beta)$ of a purely atomic contribution, for instance given by the phenomenological expression (II.27) of $Z_\mathrm{H}^{(\mathrm{scr})}$ or by the Planck-Larkin formula [55], remains arbitrary. We stress that such arbitrariness does not cause any trouble here, since only the full contribution embedded in $\alpha_3(\beta)$ is relevant for thermodynamics.

Eventually, notice that ordinary virial expansions in powers of ρ at fixed T [56–59], can be easily recovered from SLT expansion (III.38) by expanding coefficients $b_k(\rho/\rho^*)$ in powers of ρ/ρ^*. This has been explicitely checked up to order ρ^2, by noting that partition functions $Z(1,1)$, $Z(2,0)$ and $Z(0,2)$ are merely related to two-body quantum virial functions first introduced by Ebeling [56].

2. Particle correlations

The SCR also provides diagrammatical series for equilibrium particle correlations, $\rho^{(\mathrm{T})}_{\alpha_\mathrm{a}\alpha_\mathrm{b}}(\mathbf{r}_\mathrm{a},\mathbf{r}_\mathrm{b}) = \rho^{(2)}_{\alpha_\mathrm{a}\alpha_\mathrm{b}}(\mathbf{r}_\mathrm{a},\mathbf{r}_\mathrm{b}) - \rho_{\alpha_\mathrm{a}}\rho_{\alpha_\mathrm{b}}$, where graphs are similar to those introduced above for particle densities [50]. Not surprisingly, the asymptotical behaviour of $\rho^{(\mathrm{T})}_{\alpha_\mathrm{a}\alpha_\mathrm{b}}(\mathbf{r}_\mathrm{a},\mathbf{r}_\mathrm{b})$ when $R = |\mathbf{r}_\mathrm{a} - \mathbf{r}_\mathrm{b}| \to \infty$, is determined by the large-distance behaviour of bonds $\mathcal{F}_\phi$. It turns out that bonds $-\beta\Phi$, which might give *a priori* $1/R^3$-contributions, ultimately provide short-range terms thanks to the rotational invariance of statistical weights of particle clusters combined to the harmonicity of Coulomb potential [60]. On the contrary, bonds $\beta^2\Phi^2/2!$ provide $1/R^6$-contributions which do not cancel out. Thus, according to that graph by graph analysis [60], all particle correlations are expected to decay as $1/R^6$ when $R \to \infty$, namely

$$\rho^{(\mathrm{T})}_{\alpha_\mathrm{a}\alpha_\mathrm{b}}(\mathbf{r}_\mathrm{a},\mathbf{r}_\mathrm{b}) \sim \frac{A_{\alpha_\mathrm{a}\alpha_\mathrm{b}}(\beta,\rho)}{R^6} \ , \tag{III.39}$$

whith temperature- and density-dependent amplitudes $A_{\alpha_\mathrm{a}\alpha_\mathrm{b}}(\beta,\rho)$.

In the Saha regime, amplitudes $A_{\alpha_\mathrm{a}\alpha_\mathrm{b}}(\beta,\rho)$ can be determined within the method used for deriving the SLT expansion of the pressure (III.38). Here, it is important to select first the graphs which contribute to the $1/R^6$-tails, and afterwards to take the scaled low-density and low-temperature limit of the corresponding contributions. That order of limits ensures that collective screening effects arising from ionized protons and ionized electrons are indeed taken into account. Notice that Debye screening length λ_D associated with those almost classical ionized charges diverges in the SLT limit.

Within above procedure, SLT expansions of $A_{\alpha_\mathrm{a}\alpha_\mathrm{b}}(\beta,\rho)$ can be derived [60]. At leading order, $A_{\mathrm{pp}}(\beta,\rho)$ reduces to a quadratic form in the ideal densities (III.10) of (III.11) of ionized protons and hydrogen atoms respectively,

$$A_{\mathrm{pp}}(\beta,\rho) = \rho^{(\mathrm{id})}_{\mathrm{at}}\rho^{(\mathrm{id})}_{\mathrm{at}}C_{\mathrm{at-at}}(T) + \rho^{(\mathrm{id})}_{\mathrm{p}}\rho^{(\mathrm{id})}_{\mathrm{at}}C_{\mathrm{p-at}}(T) + \rho^{(\mathrm{id})}_{\mathrm{at}}\rho^{(\mathrm{id})}_{\mathrm{p}}C_{\mathrm{at-p}}(T) + ... \tag{III.40}$$

where terms left over decay exponentially faster than $(\rho^*)^2$. That structure is easily interpreted by noting that each proton in correlation $\rho^{(\mathrm{T})}_{\mathrm{pp}}$ may be either ionized or recombined into an atom. Then, the insertion of that leading quadratic structure

of amplitudes in asymptotical behaviour (III.39) provides a natural definition of effective potentials between ionized charges and atoms. In particular, the atom-atom effective interaction is

$$U_{\rm at-at}^{\rm (eff)}(R) = -\frac{k_{\rm B}T\, C_{\rm at-at}(T)}{R^6}\ . \tag{III.41}$$

Taking into account the expression of $C_{\rm at-at}(T)$ derived in Ref. [60], and definition (II.30) of van der Waals potential, that effective interaction can be rewritten as

$$U_{\rm at-at}^{\rm (eff)}(R) = \left(1 - c_{\rm at}\frac{k_{\rm B}T}{|E_{\rm H}|}\right)\ U_{\rm vdW}(R) \tag{III.42}$$

where $c_{\rm at}$ is a numerical positive constant. Thus, atom-atom van der Waals interactions are not perfectly screened by free charges, which only reduce their amplitude, in qualitative agreement with heuristic arguments presented in Section II D. Remarkably, reduction factor $(1 - c_{\rm at}k_{\rm B}T/|E_{\rm H}|)$ does not depend on the proportion of free charges, since positive constant $c_{\rm at}$ can be expressed in terms of the sole atomic spectrum [60]. The density of free charges only intervenes in Debye screening length $\lambda_{\rm D}$, while formula (III.42) holds for $R \gg \lambda_{\rm D}$. Notice that, in the window $a_{\rm B} \ll R \ll \lambda_{\rm D}$, $U_{\rm at-at}^{\rm (eff)}(R)$ does reduce to $U_{\rm vdW}(R)$ apart from exponentially small corrections with T arising from atomic excited states [60].

F. Conclusion

According to the exact results described here, and also to other works in the literature, the present state of the art for the various issues about screening, recombination and van der Waals forces is summarized below, together with some comments about related open problems. Part of those results are described in Ref. [61] where exact results for Coulomb systems at low density are reviewed.

- *Debye exponential screening is destroyed by quantum fluctuations*

Quantum fluctuations of positions generate instantaneous electrical dipoles which cannot be perfectly screened by the surrounding plasma because of their dynamical character. Fluctuations of the resulting $1/R^3$-dipolar effective interactions ultimately pollute equilibrium particle correlations with $1/R^6$-algebraic tails. Such fluctuations are not taken into account in usual mean-field theories, like Thomas-Fermi

or RPA, which erroneously predict an exponential decay [62, 63]. Previous mechanism, intrinsic to quantum mechanics, is present in any thermodynamical state. Explicit perturbative calculations of $1/R^6$-tails have been performed in regimes where free charges behave almost classically [60, 64], for which such tails appear at distances $R \gg \lambda_{\rm D}$. Also, it has been shown [65], through a non-perturbative analysis, that the effective potential between two quantum charges immersed in a classical plasma does decay as $1/R^6$. Thus, all those results strongly suggest the breakdown of exponential screening, although a rigorous derivation is not yet available.

Besides a proof of algebraic screening, explicit calculations of algebraic tails in strongly degenerate plasmas remain to be done. In particular, such calculations might be quite useful in condensed matter, where effective electron-electron interactions are oftenly modelized as Dirac delta functions in order to account for screening [85].

• *Recombined entities must be defined in a double zero-density and zero-temperature limit*

In agreement with simple findings, contributions to thermodynamical quantities of familiar chemical species, emerge unambiguously when both density and temperature vanish. The Screened Cluster Representation, which can be devised for any mixture of nuclei and electrons [50], is a suitable theoretical framework for evaluating such contributions. As it can be naively expected, when $T \to 0$, the leading contribution of a given recombined entity is controlled by the Boltzmann factor associated with its groundstate energy in the vacuum. At finite temperatures, contributions from thermal excitations of that entity, and from its dissociation products and their screened interactions, are all mixed together. This is well illustrated by the analysis of the equation of state of hydrogen in the Saha regime [53].

In approaches based on the chemical picture, the choice of a suitable internal partition function for recombined species is a central question, which has been the source of many controversies since the introduction of Planck-Larkin formula (see e.g. Refs. [66–68]). As far as thermodynamical quantities are concerned, the analysis of the various contributions in their SCR confirms the arbitrariness of such a choice.

More interesting, that analysis shows that, in phenomenological theories, the internal partition function of a given chemical species, should be defined simultaneously with the related contributions of its elementary components. The SCR itself might serve as an useful guide for introducing suitable modelized ingredients in chemical approaches.

• *Free charges reduce the amplitude of van der Waals interactions*

In the framework of the many-body problem, it is natural to define effective potentials between recombined entities from the asymptotic large-distance behaviour of equilibrium correlations between their elementary components. Since all particle correlations decay as $1/R^6$, effective interactions between neutral or charged entities also decay *à la van der Waals* as $1/R^6$. The corresponding amplitudes are controlled by quantum fluctuations of electrical dipoles, the size of which is typically of order either the Bohr radius $a_{\rm B}$ for recombined charges or thermal de Broglie wavelengths for free charges. Thus, genuine van der Waals interactions between atoms or molecules are not perfectly screened by free charges, as a consequence of the breakdown of Debye exponential screening.

Free charges should reduce the amplitude of van der Waals interactions, as suggested by the exact calculation for hydrogen in the Saha regime. At sufficiently low temperatures and low densities, the corresponding renormalization factor does not depend on ρ, and is linear in T. It should be quite instructive to compare that first-principles prediction to that of phenomenological approaches like Lifchitz theory [69–72]. Also, the SCR of particle correlations should provide some insights for reliable estimations of previous reduction factor at higher temperatures and densities. The reduction of the amplitude of van der Waals interactions by free charges might have important consequences on the phase diagrams, as quoted in Ref.[73] for a system of biological macromolecules immersed in an highly concentrated salt.

---

[1] G. Gouy, Sur la constitution de la charge électrique à la surface d'un électrolyte, *J. Phys. Théor. Appl.* **9**:457 (1910)

[2] D.L. Chapman, A contribution to the theory of electrocapillarity, *Lond. Edinb. Dubl. Phil. Mag.* **25**:475 (1913)

[3] P. Debye and E. Hüuckel, Zur theory der elektrolyte, *Z. Phys.* **24**:185-206 (1923)

[4] M. Kac, G.E. Uhlenbeck and P.C. Hemmer, On van der Waals theory of vapor-liquid equilibrium. 1. Discussion of an one-dimensional model, *J. Math. Phys.* **4**:216 (1963)

[5] J. Barré, Mécanique statistique et dynamique hors équilibre de systèmes avec interactions à longue portée, PhD thesis ENS Lyon (2003), http://tel.archives-ouvertes.fr/tel-00430889/fr/

[6] A. Alastuey, M. Magro and P. Pujol, Physique et outils mathématiques : méthodes et exemples (Éditions du CNRS, EDP Sciences, 2008)

[7] D.C. Brydges and P. Federbush, Debye screening, *Commun. Math. Phys.* **73**:197 (1980)

[8] J. Imbrie, Debye screening for jellium and other Coulomb systems, *Commun. Math. Phys.* **87**:515 (1983)

[9] T. Kennedy, Meanfield theory for Coulomb systems *J. Stat. Phys.* **37**:529 (1984)

[10] A. Alastuey and Ph.A. Martin, Decay of correlations in classical fluids with long range forces, *J. Stat. Phys.* **39**:405 (1985)

[11] Ph.A. Martin, Sum rules in charged fluids, *Rev. Mod. Phys.* **60**:1075-1127 (1988)

[12] A. Campa, T. Dauxois and S. Ruffo, Statistical mechanics and dynamics of solvable models with long range interactions, *Phys. Rep.* **480**:57-159 (2009)

[13] Y. Pomeau, Statistical mechanics of gravitational plasmas, in *Second Warsaw School of Statistical Physics*, edited by B. Cichoski, M. Napiórkowski and J. Piasecki (Warsaw University Press, 2008)

[14] R. Abe, Giant cluster expansion theory and its application to high temperature plasma, *Prog. Theor. Phys.* **22**:213 (1959)

[15] E. Meeron, Theory of potentials of average force and radial distribution function in ionic solutions, *J. Chem. Phys.* **28**:630-643 (1958); Plasma Physics (McGraw-Hill, New York, 1961)

[16] J.N. Aqua and M. Fisher, Ionic criticality : an exactly soluble model, *Phys. Rev. Lett.* **92**:135702-1 (2004)

[17] L.H. Thomas, The calculation of atomic fields, *Proc. Cambridge Phil. Soc.* **23**:542-548

(1927)

[18] E. Fermi, Un Metodo Statistico per la Determinazione di alcune Priorieta dell'Atome, *Rend. Accad. Naz. Lincei* **6**:602-607 (1927)

[19] N.W. Ashcroft and N.D. Mermin, Solid state physics (Saunders College Publishing, Orlando, 1976)

[20] A.L. Fetter and J.D. Walecka, Quantum theory of many particle systems (McGraw-Hill, New York, 1971)

[21] C. Kittel, Introduction to solid state physics (Wiley and Sons, New York-London-Sydney, 1967)

[22] D.C. Brydges and E. Seiler, Absence of screening in certain lattice gauge and plasma models, *J. Stat. Phys.* **42**:405 (1986)

[23] A. Alastuey and Ph. A. Martin, Absence of exponential clustering for static quantum correlations and time-displaced correlations in charged fluids, *Eur. Phys. Lett.* **6**:385-390 (1988)

[24] M. Saha, *Philos. Mag.* **40**:472 (1920)

[25] F. London, Theory and systematics of molecular forces, *Z. Phys.* **63**:245-279 (1930)

[26] L. Schiff, Quantum Mechanics (McGraw-Hill, New York, 1968)

[27] B. Derjaguin and L. Landau, Theory of the stability of strongly charged lyophobic sols and the adhesion of strongly charged particles in solutions of electrolytes, *Acta Physica Chemica URSS* **14**:633 (1941)

[28] E.J.W. Verwey and J.Th.G. Overbeek, Theory of the stability of lyophobic colloids (Elsevier, Amsterdam,1948)

[29] J. Israelachvili, Intramolecular and surface forces (Academic, New York, 1995)

[30] E.H. Lieb and J. Lebowitz, The constitution of matter: existence of thermodynamics for systems composed of electrons and nuclei, *Adv. Math.* **9**: 316-398 (1972)

[31] F. Dyson and A. Lenard, Stability of matter I, *J. Math. Phys.* **8**:423-434 (1967); Stability of matter II, *J. Math. Phys.* **9**:698-711 (1968)

[32] N. Macris and Ph.A. Martin, Ionization equilibrium in the proton-electron gas, *J. Stat. Phys.* **60**:619-637 (1990)

[33] J.G. Conlon, E.H. Lieb and H.T. Yau, The Coulomb gas at low temperature and low density, *Commun. Math. Phys.* **125**:153-180 (1989)

[34] C. Fefferman, The atomic and molecular nature of matter, *Rev. Math. Iberoamericana* **1**:1-44 (1985)

[35] B. Simon, Functional Integration and Quantum Physics (Academic, New York, 1979)

[36] L.S. Schulman, Techniques and Applications of Path Integrals (Wiley, New York, 1981)

[37] G. Roepstorff, Path Integral Approach to Quantum Physics (Springer, Berlin, 1994)

[38] H. Kleinert, Path Integrals in Quantum Mechanics, Statistics, Polymer Physics and Financial Markets (World Scientific, 2004)

[39] R.P. Feynman and A.R. Hibbs, Quantum mechanics and path integrals, (McGraw-Hill, New York, 1965)

[40] E.P. Wigner, *Phys. Rev.* **40**:749 (1932)

[41] J.G. Kirkwood, *Phys. Rev.* **44**:31 (1933); *Phys. Rev.* **45**:116 (1934)

[42] L.D. Landau and E.M. Lifchitz, Quantum mechanics, vol.5 of the course of Theoretical Physics (Pergamon Press, Oxford, 1958)

[43] S. Paulin, A. Alastuey and T. Dauxois, Analysis of path integrals at low temperature : box formula, occupation time and ergodic approximation, *J. Stat. Phys.* **128**:1391-1414 (2007)

[44] J. Ginibre, Some applications of functional integration in statistical mechanics, in *Statistical Mechanics and Quantum Field Theory*, edited by C. DeWitt and R. Stora (les Houches, Gordon and Breach, 1971)

[45] F. Cornu, Correlations in quantum plasmas: I. Resummations in Mayer-like diagrammatics, *Phys. Rev. E* **53**:4562 (1996)

[46] Ph.A. Martin, Quantum Mayer graphs: applications to Bose and Coulomb gases, *Acta Physica Polonica B* **34**:3629 (2003)

[47] Ph.A. Martin and J. Piasecki, Self-consistent equation for an interacting Bose gas, *Phys. Rev. E* **68**:016113 (2003); Bose gas beyond mean field *Phys. Rev. E* **71**:016109 (2005)

[48] J.E. Mayer and E.W. Montroll, Molecular distributions *J. Chem. Phys.* **9**:2-16 (1941)

[49] J.P. Hansen and I.R. Mc Donald, Theory of simple liquids (Academic Press, London, 1986)

[50] A. Alastuey, V. Ballenegger, F. Cornu and Ph.A. Martin, Screened cluster expansions

for partially ionized gases, *J. Stat. Phys.* **113**:455-503 (2003)

[51] F.J. Rogers, Statistical mechanics of Coulomb gases of arbitrary charge, *Phys. Rev. A* **10**:2441 (1974)

[52] V. Ballenegger, Ph.A. Martin and A. Alastuey, Quantum Mayer graphs for Coulomb systems and the analog of the Debye potential, *J. Stat. Phys.* **108**:169-211 (2002)

[53] A. Alastuey, V. Ballenegger, F. Cornu and Ph.A. Martin, Exact results for thermodynamics of the hydrogen plasma: low-temperature expansions beyond Saha theory, *J. Stat. Phys.* **130**:1119-1176 (2008)

[54] A. Alastuey and V. Ballenegger, Exact asymptotic expansions for thermodynamics of hydrogen gas in the Saha regime, *J. Phys. A : Math. Theor.* **42**:214031 (2009)

[55] A.I. Larkin, *Zh. Eksp. Teor. Fiz.* **38**:1896 (1960); *Soviet Phys. JETP* **11**:1363 (1960)

[56] W. Ebeling, *Ann. Phys. Leipzig* **19**:104 (1967)

[57] W.D. Kraeft, D. Kremp, W. Ebeling, and G. Ropke, Quantum Statistics of Charged Particle Systems (Plenum Press, New York, 1986)

[58] A. Alastuey and A. Perez, Virial expansion of the equation of state of a quantum plasma, *Europhys. Lett.* **20**:19-24 (1992)

[59] T. Kahlbaum, The quantum-diffraction term in the free energy for Coulomb plasma and the effective-potential approach, *J. Phys. IV* **10**(P5):455 (2000).

[60] A. Alastuey, F. Cornu and Ph. A. Martin, Van der Waals forces in presence of free charges: an exact derivation from equilibrium quantum correlations, *J. Chem. Phys.* **127**:054506 (2007)

[61] D.C. Brydges and Ph.A. Martin, Coulomb systems at low density : a review, *J. Stat. Phys.* **96**:1163-1330 (1999)

[62] A. Alastuey, Breakdown of Debye screening in quantum Coulomb systems and van der Waals forces, *Physica A* **263**:271-283 (1999)

[63] F. Cornu and Ph.A. Martin, Electron gas beyond the random phase approximation : algebraic screening, *Phys. Rev. A* **44**:4893 (1991)

[64] F. Cornu, Exact algebraic tails of static correlations in quantum plasmas at low density, *Phys. Rev. Lett.* **78**:1464 (1997)

[65] A. Alastuey and Ph.A. Martin, Absence of exponential clustering in quantum Coulomb fluids, *Phys. Rev. A* **40**:6485-6520 (1989)

[66] I.L. Iosilevski and V.K. Gryaznov, Comparative accuracy of thermodynamic description of properties of a gas plasma in the Thomas-Fermi and Saha approximations, *High Temp.* **19**:799 (1981)

[67] A.S. Kaklyugin and G.E. Norman, Thermodynamic functions (analytic expressions) for partially ionized strongly coupled plasmas. Bound and free states contributions, *Journal de Physique IV* **10**:153 (2000)

[68] A.N. Starostin and V.C. Roerich, Bound states in non-ideal plasmas : formulation of the partition function and application to the solar interior, *Plasma Sources Sci. Technol.* **15**:410-415 (2006); Equation of state of weakly non-ideal plasmas and electroneutrality condition, *J. Phys. A : Math. Theor.* **39**:4431-4439 (2006)

[69] E.M. Lifchitz, *Soviet Phys. JETP* **2**:73 (1956)

[70] L.D. Landau and E.M. Lifchitz, Electrodynamics of continuous media, vol.8 of the course of Theoretical Physics (Pergamon Press, Oxford, 1960)

[71] J. Mahanty and B.W. Ninham, Dispersion forces (Academic, New York, 1976)

[72] V.A. Parsegian, Van der Waals forces : a handbook for biologists, chemists, engineers and physicists (Cambridge University Press, Cambridge, 2005)

[73] H.I. Petrache, S. Tristram-Nagle, D. Harries, N. Kucerka, J.F. Nagle and V.A. Parsegian, Swelling of phospholipids by monovalent salt, *J. Lipid Res.* **47**:302 (2006)

[74] When quantum effects become important, k_BT is no longer the relevant energy which determines the average speed of the considered charge. For instance, conduction electrons in metals are highly degenerate and we have to compare the Fermi energy to mc^2.

[75] See for instance a one-dimensional classical gas where the attractive part of the pair-potential has an infinite range and a vanishingly small amplitude [4], or lattice systems described by Ising Hamiltonians where any two spins interact with a constant and vanishingly small coupling (see e.g. Ref. [5]). In those double zero-coupling and infinite-range limits, the mean-field treatment becomes exact.

[76] In systems where particles interact *via* the gravitationnal $1/r$-potential, since all masses are positive, all particles attract each other so no screening occurs [12, 13].

[77] Also, in the present calculation, we omit all effects present in real condensed matter, like those arising from either the band structure of the electronic spectrum, or the

electron-phonon coupling [19, 21]. Despite its obvious drawbacks, Thomas-Fermi calculation suggests that the electron-electron effective potential is shorter ranged than the bare Coulomb interaction.

[78] The fractions of atoms and molecules can be determined within a simplified mixture model of non-interacting classical particles with an internal energy E_{H_2} or E_{H}. The corresponding minimization equation then reduces to the usual mass action law associated with dissociation reaction $\mathrm{H}_2 \rightleftharpoons 2\mathrm{H}$.

[79] That standard definition of the grand-canonical ensemble may be viewed as rather artificial in the sense that Dirichlet boundary conditions do not describe the physical situation which is considered in the Gibbs construction, where particles can freely go in and out the volume Λ immersed inside a much larger container. Nevertheless, in the thermodynamic limit $\Lambda \to \infty$, boundary conditions become irrelevant for bulk quantities. Therefore, for our purpose it is legitimate to use definition (III.2), where particle numbers are varied by some hidden operator.

[80] In fact, those inequalities have been conjectured by Fefferman [34], but they are not yet proved. However, all the known groundstate energies of recombined entities with few protons and electrons do satisfy such inequalities.

[81] Of course, inequality (III.13) also intervenes in the determination of the chemical composition of hydrogen *via* the minimization procedure described in Section II D. It indeed ensures that atoms are the proeminent chemical species at sufficiently low densities for a given low temperature.

[82] Quantum corrections to classical formula (III.19) can be expanded in powers of $\hbar^2$ according to the well-known Wigner-Kirkwood expansion [40–42]. That expansion can be easily retrieved within FK representation (III.15), by expanding time-average (III.18) in power series of $\lambda\boldsymbol{\xi}$ and by applying Wick theorem to the calculation of the resulting moments of $\boldsymbol{\xi}$.

[83] This can be checked by replacing all loop interactions by their static parts in chain sum (III.32). The corresponding integration over loop internal degrees of freedom involved in each $\mathrm{d}\mathcal{L}_i$ provides the square of some wavenumber κ_{loop}. The chain sum then becomes a geometrical series in $-\kappa_{\mathrm{loop}}^2/k^2$ in Fourier space, and the resulting static part of the effective potential involves factor $\exp(-\kappa_{\mathrm{loop}}|\mathbf{X}_{\mathrm{a}} - \mathbf{X}_{\mathrm{b}}|)$.

[84] Since ionized protons and ionized electrons behave almost classically in the Saha regime, contributions of screened interactions are controlled by Debye length associated with the corresponding density of those charges. Notice that screened potential $e_{\alpha_a} e_{\alpha_b} \phi(\mathcal{L}_a, \mathcal{L}_b)$ precisely decays as $q_a e_{\alpha_a} q_b e_{\alpha_b} \exp(-\kappa_D |\mathbf{X}_a - \mathbf{X}_b|)/|\mathbf{X}_a - \mathbf{X}_b|$ at distances $|\mathbf{X}_a - \mathbf{X}_b|$ of order λ_D. The algebraic $1/|\mathbf{X}_a - \mathbf{X}_b|^3$-decay of ϕ takes place at distances $|\mathbf{X}_a - \mathbf{X}_b|$ much larger than λ_D [53].

[85] Such a modelization of screening of Coulomb interactions between electrons, may be sufficient for interpreting rather complicated phenomena mainly driven by other mechanisms. Nevertheless, the existence of long-ranged normal attractive interactions between electrons might induce some observable consequences. For instance, in normal superconductivity, interactions generated *via* the electron-phonon coupling are believed to be responsible for the formation of Cooper pairs.